VII International School-Conference "Promising multicomponent ("high entropic") materials", dedicated to the 100th anniversary of Yuri Alexandrovich Skakov
October 06-10, 2025 г.

№ 3.2

nek6@tpu.ru

STUDY OF HYDROGEN PROPERTIES OF TIFE METAL HYDRIDE ALLOY WITH PARTIAL SUBSTITUTION OF FE WITH CR

N.E. Kurdyumov, E.D. Anzhigatova
National Research Tomsk Polytechnic University, Tomsk, Russia

The synthesis of $TiFe_{0.95}Cr_{0.05}$, $TiFe_{0.9}Cr_{0.1}$, $TiFe_{0.8}Cr_{0.2}$, $TiFe_{0.8}Cr_{0.1}$, $TiFe_{0.7}Cr_{0.2}$ was carried out by electric arc melting at 200 A, 220 A and 240 A.
Dispersion in a hydrogen environment at P = 30 bar, T = 30 °C.
Activation was in a hydrogen atmosphere 30 bar at 30°C for 60 minutes.

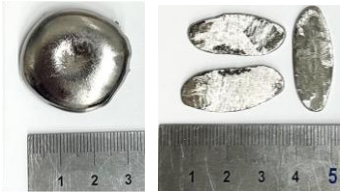

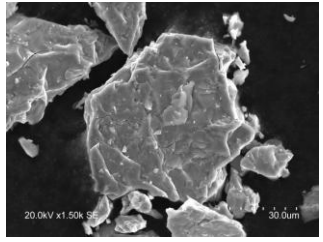

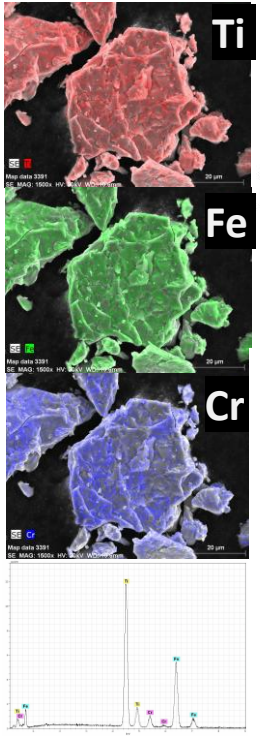

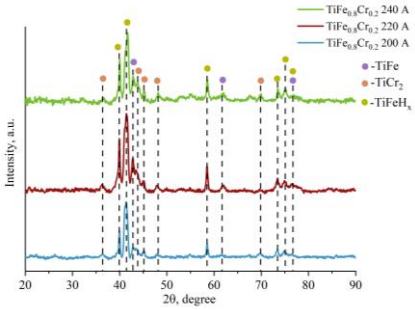

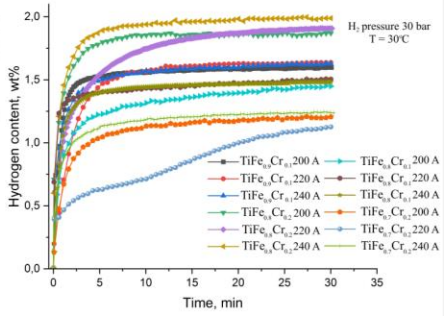

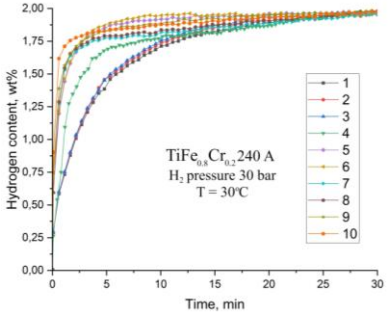

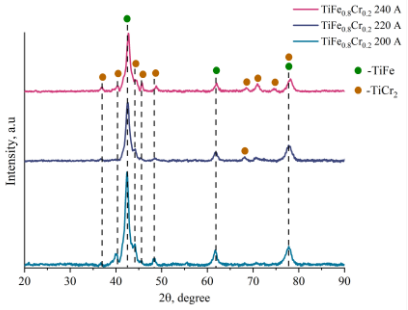

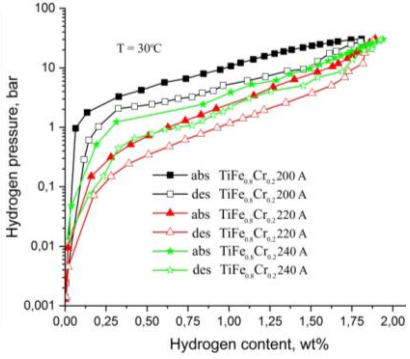

The addition of Cr is characterized by the precipitation of a secondary phase on the alloy surface, therefore hydrogen sorption begins from the first cycle (30 bar, 30°C). The hydrogen capacity of Ti-Fe-Cr alloys with different stoichiometric compositions ranges from 1 to 1.95 wt.%. The partial replacement of Fe with Cr in TiFe-based alloys improves the kinetics of hydrogen sorption/desorption by creating active sites for hydrogen dissociation on the alloy surface.

VII International School-Conference "Promising multicomponent ("high entropic") materials", dedicated to the 100th anniversary of Yuri Alexandrovich Skakov
October 06-10, 2025 г.

№ 3.3

rre1@tpu.ru

EFFECT OF NANO-NICKEL AND CARBON NANOTUBES ADDITION ON HYDROGEN STORAGE PROPERTIES OF MAGNESIUM HYDRIDE

R.R. Elman, A. Kenzhiyev
National Research Tomsk Polytechnic University, Tomsk, Russia

The synthesis of MgH_2–20 wt.% EEWNi– 5 wt.% CNT composite was carried out in a planetary ball mill in grinding jars at a rotation speed 900 rpm for 60 min with EEWNi and 300 rpm for 180 min with CNT.
For the synthesis of the composite, MgH_2 with a hydride content of about 97 vol.% and a metallic magnesium phase content of 3 vol.% was obtained by hydrogenation from the gas phase at a temperature of 400 °C and a pressure of 30 atm H_2.

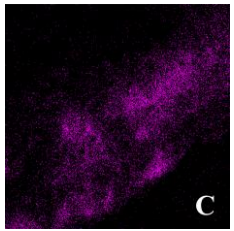

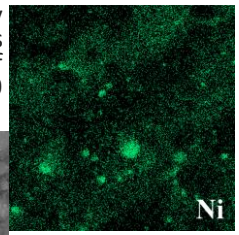

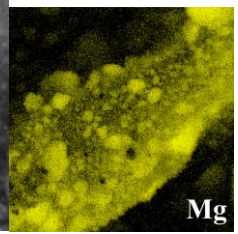

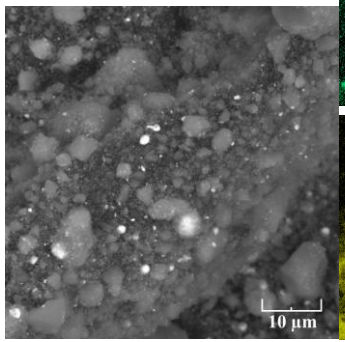

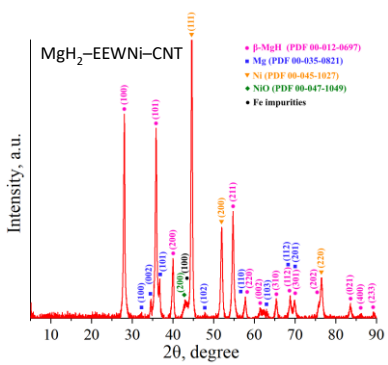

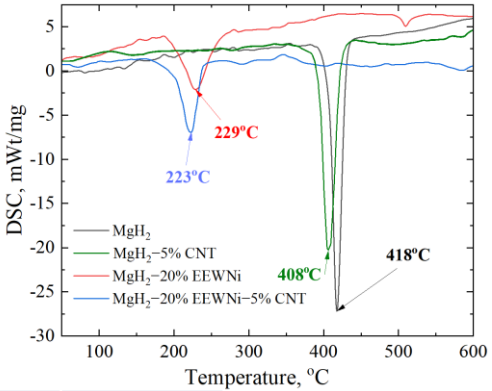

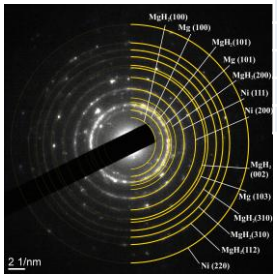

MgH2–EEWNi–CNT

Material	H_2 content, wt.%
MgH_2	6.7
MgH_2–CNT	5.5
MgH_2–EEWNi	5.6
MgH_2–EEWNi–CNT	4.3

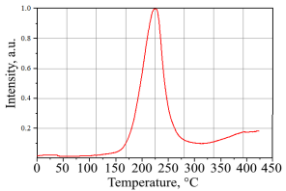

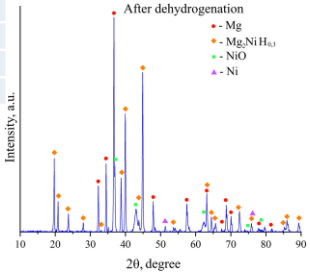

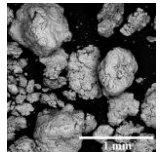

With CNT

Without CNT

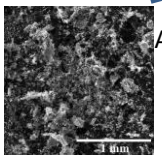

After a few reversible cycles

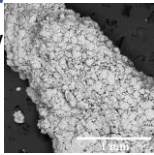

The synthesis resulted in a core-shell structure, with magnesium hydride particles serving as the core and CNT with nickel-based nanoparticles as the shell. The composite exhibits the lowest hydrogen release temperature compared to MgH_2 and binary compounds. The improvement of properties is achieved through the "hydrogen pump" mechanism when adding EEWNi, as well as the formation of a defect structure with the addition of CNTs and inhibition of particle agglomeration during synthesis and hydrogen sorption/desorption processes.

VII International School-Conference "Promising multicomponent ("high entropic") materials", dedicated to the 100th anniversary of Yuri Alexandrovich Skakov
October 06-10, 2025 г.

№ 3.4

tk0nsta@yandex.ru

New Ternary Lanthanum Halides $La(Pd,Ga)_2$ and La_3Pd_5Ga

Telnoy K.O., Fedorayev I.I., Dunaev S.F., Gribanov A.V.
Lomonosov Moscow State University, Moscow, Russian Federation

Currently, intensive research is being conducted on intermetallic compounds (IMCs) of rare earth elements with significant electron correlations. In particular, such IMCs include R–T–X systems, where R stands for a rare-earth element, T - d-element, and X - p-element (groups 13–15). Intermetallic compounds (IMCs) in ternary R–T–X systems can exhibit specific physical properties such as the formation of Kondo lattices, heavy-fermion superconductivity, valence fluctuations, and others. In the case where the d-element is palladium, the formation of IMCs with a high Pd content (> 70 at. %) is possible, which distinguishes it from other platinum-group metals.

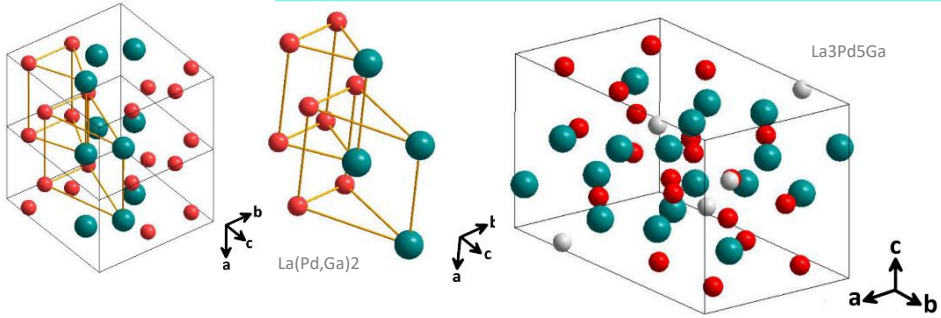

Method used

The alloys were prepared in an electric arc furnace under an argon atmosphere, followed by annealing at 800 °C in evacuated quartz ampoules using resistance furnaces for 14 days. The samples were studied using scanning electron microscopy, energy-dispersive X-ray spectroscopy, X-ray phase analysis, and differential scanning calorimetry.

Results

The existence of two new ternary compounds containing 33.3 at. % lanthanum has been established: $La(Pd,Ga)_2$, with the KHg_2-type structure (space group *Imma*), and La_3Pd_5Ga, with the Ce_3Pd_5Si-type structure (space group *Imma*). The crystal structure of the $La(Pd,Ga)_2$ phase can be described as a set of overlapping triangular. A similar structural motif is also observed in the lanthanum sublattice of the La_3Pd_5Ga compound.

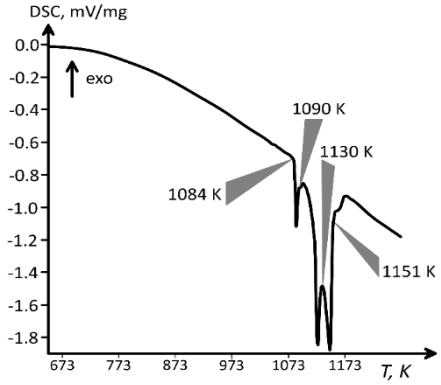

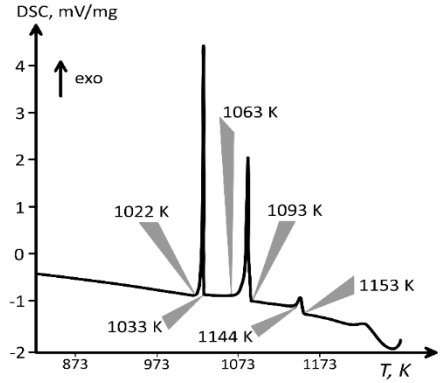

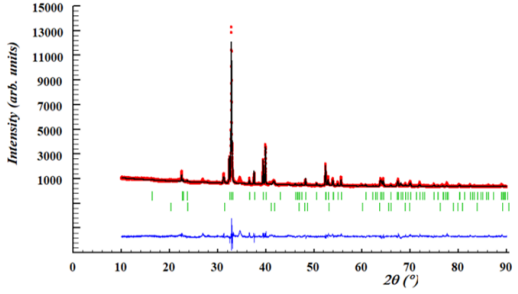

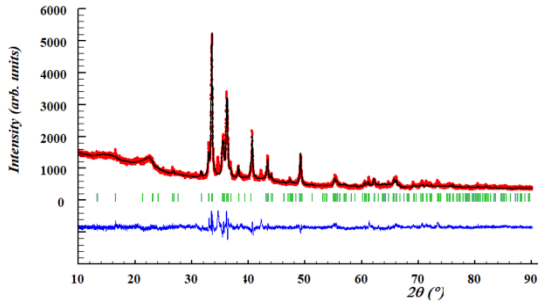

The study was conducted under the state assignment of Lomonosov Moscow State University "Fundamentals of the development of metallic and composite materials", project No. AAAA-A21-121011590083-9.

VII International School-Conference "Promising multicomponent ("high entropic") materials", dedicated to the 100th anniversary of Yuri Alexandrovich Skakov
October 06-10, 2025 г.

№ 3.5

dorofeeva525252@mail.ru

Investigation Of Amorphous Magnesium-Based Metallic Alloys Before And After Hydrogenation

[1]Dorofeeva V.A., [1]Korol A.A., [2]Berdonosova E.A., [2]Klyamkin S.N., [1]Zadorozhnyy V.Yu.
[1]National University of Science and Technology MISIS, Moscow, Russia
[2]Lomonosov Moscow State University, Moscow, Russia

Abstract

Two melt-spun amorphous Mg–Cu–Ag–Yb and Mg–Cu–Yb–Co alloys are evaluated as fillers for metal–polymer gas-separation membranes. As-prepared ribbons are fully amorphous, but hydrogenation induces crystallization, limiting reversibility. Calorimetry indicates a narrow supercooled-liquid region and multiple melting events of the crystallized phases. These results define the practical operating range and motivate composition/structure optimization to suppress crystallization and improve cycling stability.

Introduction

Hydrogen's value as a clean energy carrier depends on safe, reversible storage. Magnesium-based systems offer high capacity and low cost, but crystalline Mg requires high temperatures and exhibits slow sorption. Amorphous Mg alloys can mitigate these limitations, yet hydrogen can trigger crystallization and reduce reversibility.

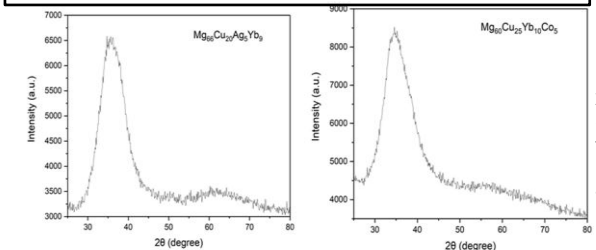

X-ray diffraction (XRD) patterns of the alloys: $Mg_{66}Cu_{20}Ag_5Yb_9$ and $Mg_{60}Cu_{25}Yb_{10}Co_5$

Methods

Amorphous melt-spun $Mg_{66}Cu_{20}Ag_5Yb_9$ and $Mg_{60}Cu_{25}Yb_{10}Co_5$ ribbons were hydrogenated. XRD before/after exposure verified amorphousness and identified crystallization/hydrides. DSC on $Mg_{66}Cu_{20}Ag_5Yb_9$ (heating/cooling) determined Tg, Tx, ΔTx, and melting events. Combined XRD/DSC assessed thermal stability and reversibility under hydrogen.

Results and Discussion

Both alloys are fully amorphous as-prepared but crystallize after hydrogenation, limiting reversibility. DSC for $Mg_{66}Cu_{20}Ag_5Yb_9$ indicates glass transition, early crystallization, a narrow supercooled-liquid region, and multiple melting steps of the crystallized phases. Together, XRD/DSC evidence points to a narrow usable temperature range and the need for composition/microstructure optimization to suppress crystallization and improve cycling stability.

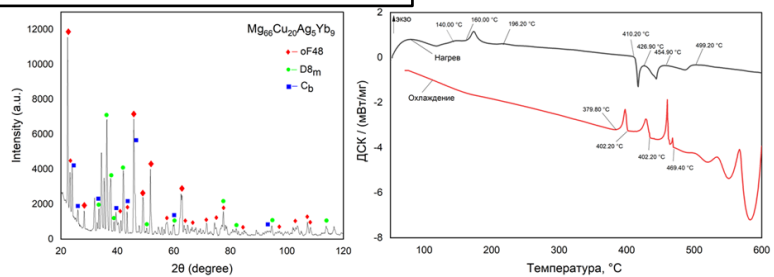

X-ray diffraction pattern of $Mg_{66}Cu_{20}Ag_5Yb_9$ after hydrogenation and differential scanning calorimetry results for the same alloy

Conclusion

Amorphous Mg–Cu–Ag–Yb and Mg–Cu–Yb–Co alloys crystallize under hydrogen and show limited thermal stability, constraining the usable temperature range. Optimizing composition and microstructure is required to suppress crystallization and improve cycling durability in membrane applications.

References

1. Zhou H. et al. Enhancement of hydrogen storage properties from amorphous Mg85Ni5Y10 alloy //Journal of non-crystalline solids. – 2023. – Т. 605. – С. 122167.
2. Jain I. P., Lal C., Jain A. Hydrogen storage in Mg: a most promising material //International journal of hydrogen energy. – 2010. – Т. 35. – №. 10. – С. 5133-5144.
3. Sadhasivam T. et al. Dimensional effects of nanostructured Mg/MgH2 for hydrogen storage applications: a review //Renewable and Sustainable Energy Reviews. – 2017. – Т. 72. – С. 523-534.

VII International School-Conference "Promising multicomponent ("high entropic") materials", dedicated to the 100th anniversary of Yuri Alexandrovich Skakov
October 06-10, 2025 г.

№ 3.6

fomin314@mail.ru

THE KOB-ANDERSEN SYSTEM CRYSTAL STRUCTURE: GENETIC ALGORITHMS VS SPONTANEOUS CRYSTALLIZATION

Yu. D. Fomin N. M. Chtchelkatchev
Institute for High Pressure Physics RAS, Troitsk, Moscow, Russia

The crystal structure of the Kob–Andersen mixture has been probed by genetic algorithm calculations. The stable structures of the system with different molar fractions of the components have been identified, and their stability at finite temperatures has been verified. It has been found that the structures of composition ABn, where n = 2, 3, or 4, can be formed in the system. Metastable structures with compositions AB0.4 and AB0.58 have also been identified. Molecular dynamics simulations of spontaneous crystallization from liquid have been performed.

Kob-Andersen (KA) model:

$$U_{LJ} = 4\varepsilon_{\alpha\beta}\left((\sigma_{\alpha\beta}/r)^{12} - (\sigma_{\alpha\beta}/r)^{6}\right),$$

$$\varepsilon_{AB}/\varepsilon_{AA} = 1.5,\ \varepsilon_{BB}/\varepsilon_{AA} = 0.5,$$

$$\sigma_{BB}/\sigma_{AA} = 0.88, \text{ and } \sigma_{AB}/\sigma_{AA} = 0.8$$

Methods:
- **USPEX variable composition calculations**
- **MD simulation of spontaneous crystallization (lammps)**

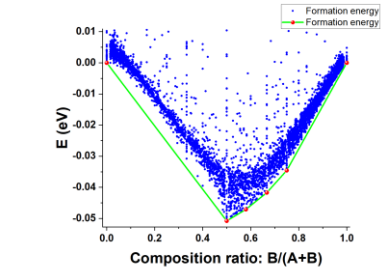

Convex hull for the KA system with different moll fraction of the components. The stars represent the location of the structures from the literature.

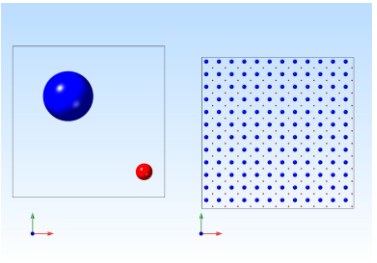

Equimolar system – CsCl structure

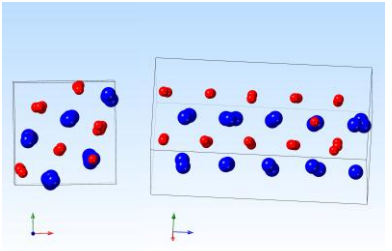

cB=0.58 – a metastable structure

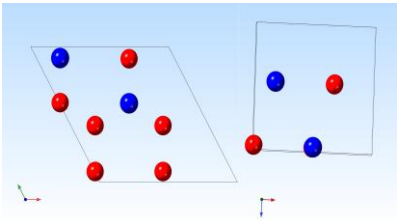

cB=3/4 – P63/mmc symmetry group; this structure is found in actinedes, for instance, AcSe3

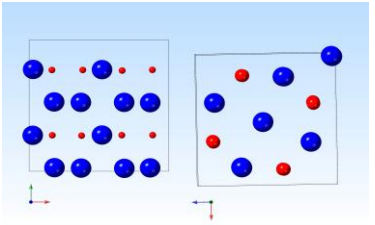

cB=0.4 – a metastable structure close to the convex hull

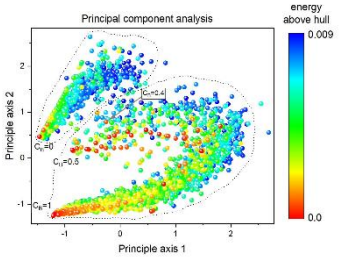

Principle components analysis of the structures. Two families of the structures are identified.

Conclusions: genetic algorithms calculations (USPEX) allowed us to find the ground state of the KA model at different concentration of the components. Only one of the predicted structures (CsCl) was known before. All the others are predicted for the first time. It was also shown that others structures, predicted mostly by educated guess are indeed metastable.

Yu. D. Fomin and N. M. Chtchelkatchev, J. Chem. Phys. 161, 204504 (2024); doi: 10.1063/5.0237306

VII International School-Conference "Promising multicomponent ("high entropic") materials", dedicated to the 100th anniversary of Yuri Alexandrovich Skakov
October 06-10, 2025 г.

№ 3.7

rusanov@uspu.ru

EFFECT OF OVERHEATING ON STRUCTURE OF FeNiBSiNb RAPIDLY QUENCHED MULTICOMPONENT ALLOY

B.A. Rusanov[1]*, V.E. Sidorov[1], P.S. Popel[1], A.I. Rusanova[2], V.I. Lad'yanov[3]

[1]Ural State Pedagogical University, Yekaterinburg, Russia

[2]N.A.Vatolin Institute of Metallurgy UB RAS, Yekaterinburg, Russia

[3]Udmurt Federal Research Center, Izhevsk, Russia

Iron- and nickel-based bulk-amorphous multicomponent alloys based are actively researched in recent years due to their distinctive mechanical and electromagnetic properties. Such materials are beginning to be used in transformer cores and other elements of electrical equipment.

$Fe_{39}Ni_{39}B_{15}Si_3Nb_4$ alloy (master alloy) was obtained in an induction furnace from pure initial components (> 99.85 at. %) after remelting for 30 min in a protective argon atmosphere. Rapidly quenched (RQ) samples in the form of rods (4 mm diameter) were obtained by suction casting.

Chemical composition of $Fe_{39}Ni_{39}B_{15}Si_3Nb_4$ alloy

Alloy	Fe, at. %	Ni, at. %	B, at. %	Si, at. %	Nb, at. %
$Fe_{39}Ni_{39}B_{15}Si_3Nb_4$	39,1 ± 0,3	38,5 ± 0,3	15,1 ± 0,1	2,5 ± 0,3	4,2 ± 0,3

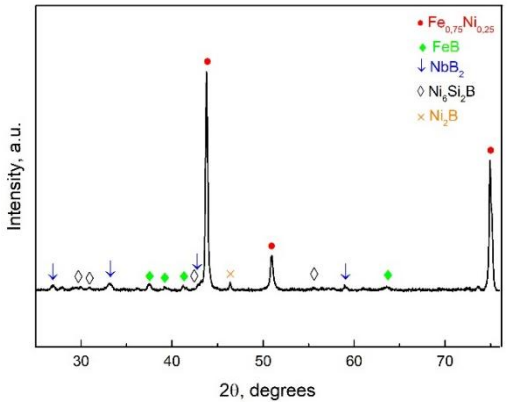

X-ray diffraction pattern of $Fe_{39}Ni_{39}B_{15}Si_3Nb_4$ master alloy

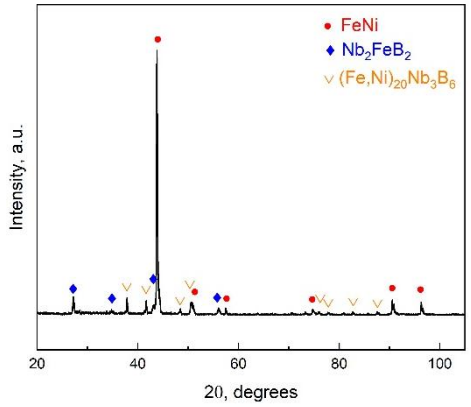

X-ray diffraction pattern of RQ $Fe_{39}Ni_{39}B_{15}Si_3Nb_4$ alloy from 1280 °C

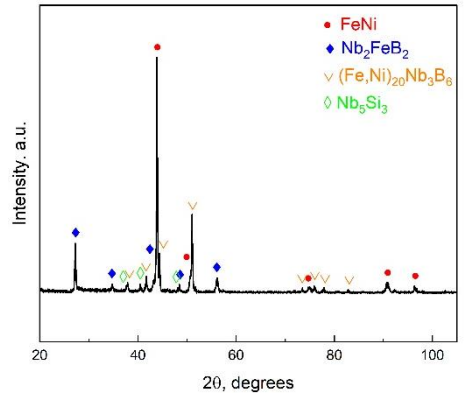

X-ray diffraction pattern of RQ $Fe_{39}Ni_{39}B_{15}Si_3Nb_4$ alloy from 1315 °C

It is found that the master alloy is multiphase, the main detected phases are $Fe_{0.75}Ni_{0.25}$, FeB, Ni_2B, $FeSi_2$. Rapid quenching of melt leads to a change in phase composition of solid samples. The main difference being the formation of the $(Fe,Ni)_{20}Nb_3B_6$ phase. At the same time significant overheating leads to a decrease in volume fraction of this phase which can reduce the glass-forming ability of the alloy.

The research was funded by the Russian Science Foundation, grant № 25-23-00049, https://rscf.ru/project/25-23-00049/

VII International School-Conference "Promising multicomponent ("high entropic") materials", dedicated to the 100th anniversary of Yuri Alexandrovich Skakov
October 06-10, 2025 г.

№ 3.8

Reem.shaheen.r.2001@gmail.com

ACTIVATED CARBON FROM COTTON WASTE FOR SUPERCAPACITOR APPLICATIONS

R. Shahin, A.O. Rodin
National University of Science and Technology MISiS, Moscow, Russia

Introduction

The growing demand for sustainable energy calls for low-cost, high-performance materials, while global cotton production generates large amounts of pre-consumer waste. These cellulose-rich residues can be converted into porous, conductive carbons with high surface area and tunable porosity. This work explores their chemical activation for eco-friendly energy storage.

Experimental part

Activated Carbon: Cotton waste was soaked in 50–85% H_3PO_4 → dried → carbonized at 600 °C → neutralized & washed → ground.
Electrodes & Supercapacitors: AC, carbon black, and PTFE (80:10:10) were mixed → filtered & rolled into sheets → cut into electrodes → assembled with separator & 1 M KNO_3.
Characterization: FT-IR , SEM, Electrochemical tests (CV, GCD, EIS).

Results and discussion

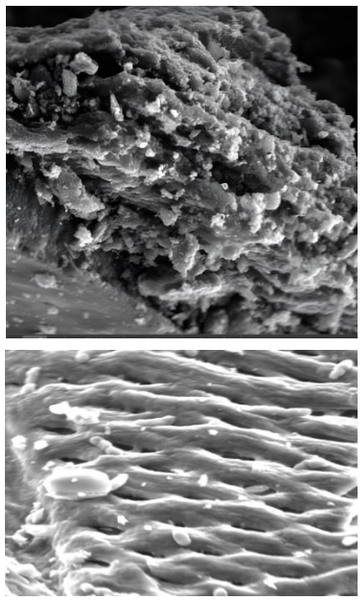

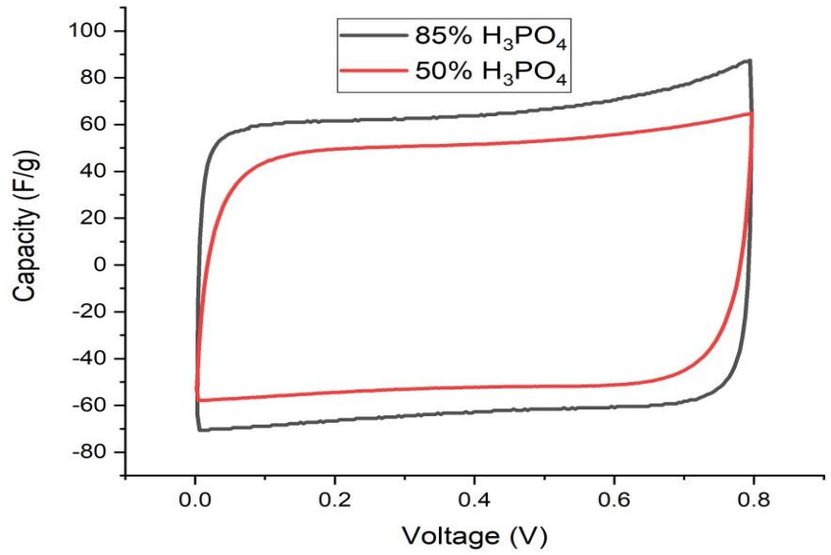

- Higher acid concentration (85%) leads to greater porosity and an interconnected framework.
- Nearly rectangular CV curves indicate ideal capacitive behavior and efficient ion transport.
- Improved morphology results in higher capacitance and enhanced electrochemical performance.
- Increased acid concentration contributes to superior supercapacitor performance.

VII International School-Conference "Promising multicomponent ("high entropic") materials", dedicated to the 100th anniversary of Yuri Alexandrovich Skakov
October 06-10, 2025 г.

davidkwartalnow@yandex.ru

The “4simplex” Plarform for predicting phase equilibria and decomposition kinetics of solid solutions in multicomponent systems (using the Co-Ti-Ta-Re system as an example)

D.V. Kvartalnov, N.E. Dmitrieva, I.I. Fedorayev

Lomonosov Moscow State University, Moscow, Russian Federation

Predicting of phase equilibria in quaternary and higher-dimensional systems is an important task for the development of advanced materials. Traditional approaches to constructing of multicomponent systems isothermal sections using graphs method by hand are extremely labor-intensive and error-prone. Moreover, the use of only isothermal sections does not allow tracking the kinetics of processes such as recrystallization, aging, and tempering, or tracking the evolution of metastable intermediate particles.

The integrated computing platform “4simplex”, developed in the course of this work, significantly accelerates and automates the key stages of the analysis of multicomponent systems and the processing of experimental data. Specialized software has been developed in the Python for constructing and visualizing isothermal sections of four-component systems in the form of tetrahedrons.

A hybrid methodology is proposed that leverages the respective strengths of diverse computational approaches:

1.Splines are employed for the smooth mathematical representation of known boundaries.

2.Arithmetic coefficients facilitate interpolation within regions lacking empirical data.

3.Triangulation is utilized to construct a continuous and topologically consistent surface model.

4.Operator adjustment capability, which effectively incorporates the human expert as a biological neural network, serving as an optimal approximator for complex, non-linear corrections.

Hand-drawn schematic

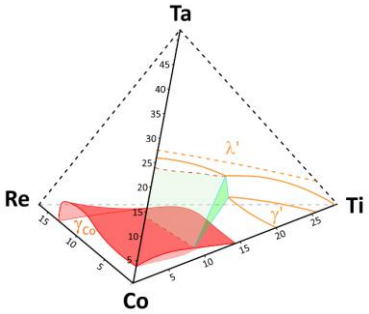

The composition point

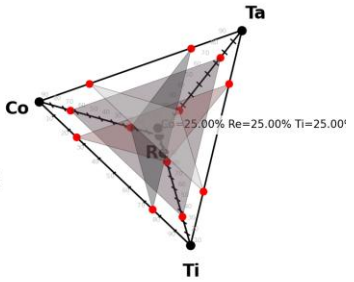

Curved surface

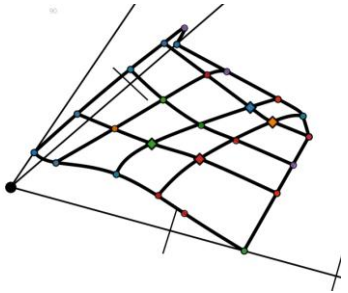

The study was conducted under the state assignment of Lomonosov Moscow State University "Fundamentals of the development of metallic and composite materials", project No. AAAA-A21-121011590083-9.

VII International School-Conference "Promising multicomponent ("high entropic") materials", dedicated to the 100th anniversary of Yuri Alexandrovich Skakov
October 06-10, 2025 г.

№ 3.10

dvt17@tpu.ru

IMPACT OF NANOSCALE Al, Cr, AND Ni ADDITIVES ON HYDROGEN DESORPTION FROM THE (001) AND (110) SURFACES OF MgH_2

D.V. Terenteva, D.B. Vrublevskii, L.A. Svyatkin
National Research Tomsk Polytechnic University, Tomsk, Russia

Введение

Поиск эффективных и экологически чистых источников энергии делает водород ключевым кандидатом благодаря его высокой энергоёмкости и экологичности. Однако основным препятствием остаётся отсутствие надёжных методов его хранения. Среди материалов особое внимание привлекает гидрид магния (MgH_2), обладающий высокой теоретической водородной ёмкостью (7,6 мас.%) и доступностью. Его использование ограничено высокой температурой десорбции (300–400 °C) и медленной кинетикой, обусловленными прочной ионной связью Mg–H. Перспективным направлением является каталитическая модификация поверхностей MgH_2 переходными металлами и лёгкими элементами (Al, Ni, Cr), способными перестраивать локальную электронную структуру без потери объёмной ёмкости. Особенно интересны поверхности (110) и (001), как наиболее и наименее энергетически устойчивые.

Цель работы: выявление влияния добавок алюминия, никеля и хрома на связи водород-добавки и водород-магний на поверхностях (001) и (110) гидрида магния.

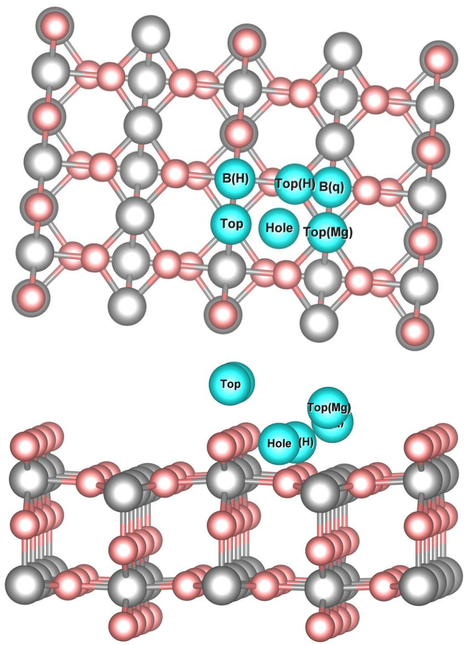

Вид сверху и вид сбору суперъячейки, моделирующей поверхность (110). *Атомы Mg, H и атомы добавок окрашены в серый, розовый и голубой цвета*

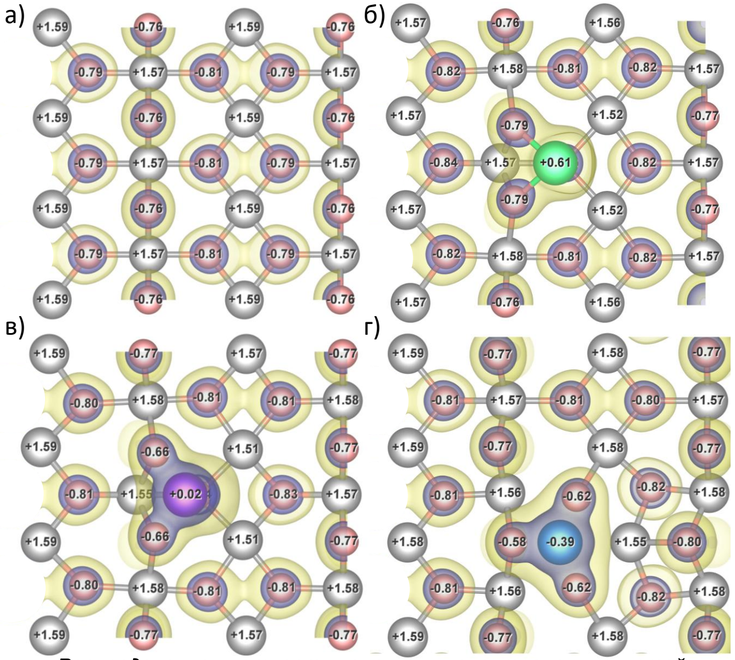

Распределение плотности валентных электронов на чистой поверхности (110) α-MgH_2 (а) и на поверхностях с адсорбированным атомом Al (б), атомом Cr (в) и атомом Ni (г). Цифры обозначают перенос заряда по Бадеру

Методы

Были выполнены расчёты из первых принципов в рамках функционала плотности методом псевдопотенциала с использованием обобщённого градиентного приближения в форме, предложенною Пердью-Бурке-Эрнценхофом.

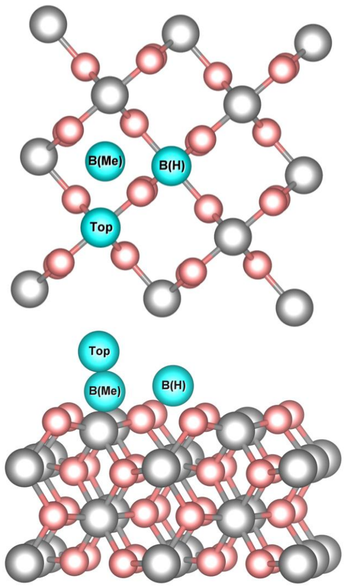

Вид сверху и вид сбору суперъячейки, моделирующей поверхность (001). Атомы Mg, H и атомы добавок окрашены в серый, розовый и голубой цвета

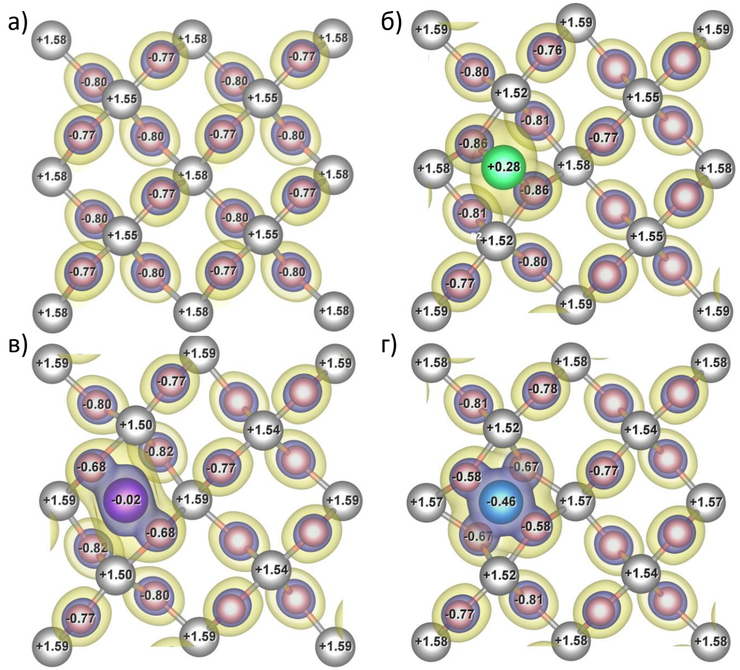

Распределение плотности валентных электронов на чистой поверхности (001) α-MgH_2 (а) и на поверхностях с адсорбированным атомом Al (б), атомом Cr (в) и атомом Ni (г). Цифры обозначают перенос заряда по Бадеру

Заключение

В исследовании установлено, что никель, хром формируют соответственно преимущественно ковалентные с ближайшими атомами водорода, а алюминий – ионно-ковалентные. Такое взаимодействие приводит к ослаблению исходных Mg–H связей, облегчая десорбцию водорода. При этом выявлено, что эффект ослабления не зависит от морфологии поверхности, а определяется исключительно типом примеси, адсорбированной на гидриде магния.

dvt17@tpu.ru

EFFECT OF Ni AND C ADDITIVES ON HYDROGEN DESORPTION FROM THE (110) SURFACE OF MgH_2

D.V. Terenteva, D.B. Vrublevskii, L.A. Svyatkin
National Research Tomsk Polytechnic University, Tomsk, Russia

Введение

Переход к возобновляемым источникам энергии делает водород ключевым энергоносителем будущего. Среди материалов для его хранения гидрид магния (MgH_2) выделяется высокой теоретической водородной емкостью (7,6 масс.%), доступностью и экологичностью. Однако его использование ограничено высокими температурами дегидрирования (300–350 °C) и медленной кинетикой сорбции/десорбции. Для решения этих проблем применяют модификации MgH_2 каталитическими и теплопроводящими добавками. В частности, никель ускоряет процессы гидрирования и дегидрирования благодаря высокой каталитической активности, а углерод повышает теплопроводность, предотвращает агломерацию частиц и способствует равномерному тепломассообмену, обеспечивая стабильность и долговечность накопителей водорода.

Цель работы: изучение синергетического эффекта влияния атомов никеля и углерода на десорбционную способность MgH_2. .

Методы

Были выполнены расчёты из первых принципов в рамках функционала плотности методом псевдопотенциала с использованием обобщённого градиентного приближения в форме, предложенною Пердью-Бурке-Эрнценхофом.

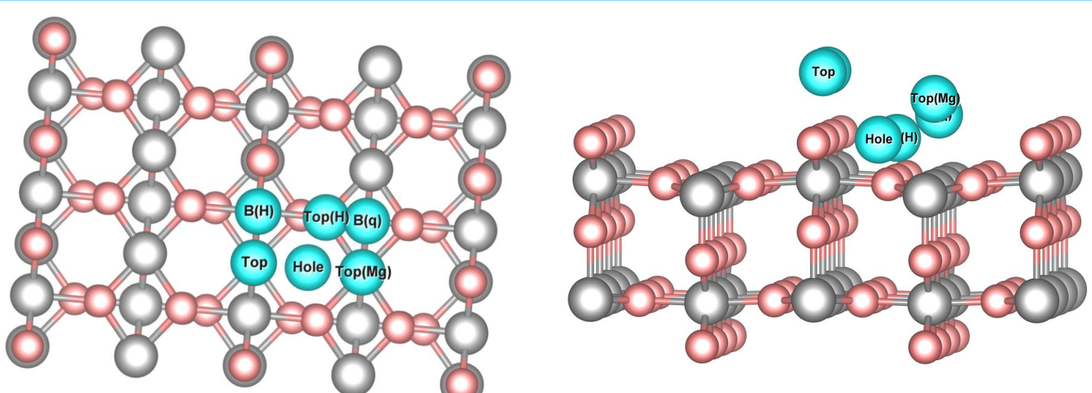

Вид сверху и вид сбору суперъячейки, моделирующей поверхность (110). *Атомы Mg, H и атомы добавок окрашены в серый, розовый и голубой цвета*

Энергии адсорбции атомов C и Ni при их различных положениях на поверхности $MgH_2(110)$

Положение Адсорбции	$E_{адс}$, эВ	
	C	Ni
B(H)	-5,02	-2,14
B(q)	-2,71	-2,37
Hole	-2,95	-0,96
Top	-6,18	-3,18
Top(H)	-1,07	-1,25
Top(Mg)	-5,63	-4,40

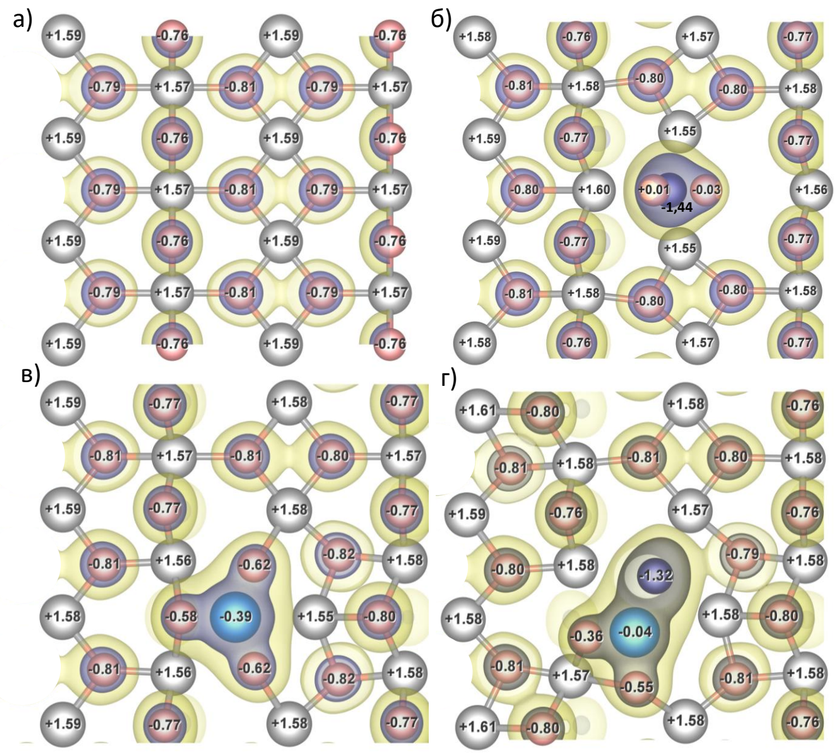

Распределение плотности валентных электронов на чистой поверхности (110) α-MgH_2 (а) и на поверхностях с адсорбированным атомом C (б), атомом Ni (в) и комплексом Ni-C (г). Цифры обозначают перенос заряда по Бадеру

Заключение

Высокая электроотрицательность углерода приводит к аккумуляции значительного отрицательного заряда, что делает его основным акцептором электронной плотности как на чистой поверхности MgH_2, так и при совместной адсорбции с Ni. При этом на ближайших к углероду атомах перенос заряда не наблюдается, что указывает на формирование слабых ковалентных связей C–H или C–Ni. Напротив, Ni не оказывает столь выраженного влияния на перераспределение электронной плотности и образует преимущественно ковалентные связи с соседними атомами водорода. В обоих случаях результатом влияния добавок Ni и C является ослабление связей Mg–H.

VII International School-Conference "Promising multicomponent ("high entropic") materials", dedicated to the 100th anniversary of Yuri Alexandrovich Skakov
October 06-10, 2025 г.

№ 3.12

abzalovdanil99@yandex.ru

SELF-PROPAGATING HIGH-TEMPERATURE SYNTHESIS OF MgAlON USING $KClO_4$ AS AN EXOTHERMIC ADDITIVE

Abzalov D.I., Akopdzhanyan T.G.
Merzhanov Institute of Structural Macrokinetics and Materials Science, Chernogolovka, Russia

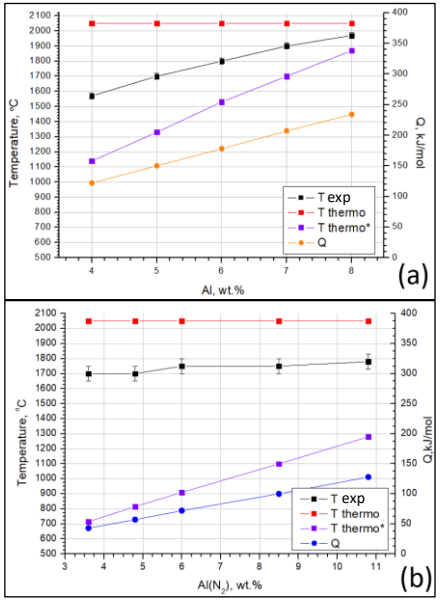

Fig. 1. Graph of the experimental combustion temperature, calculated temperature, and calculated heat release as a function of the Al content involved in the oxidation reaction (a) and nitriding reaction (b). T exp – experimental combustion temperature; T thermo – calculated combustion temperature (according to the experimental compositions); T thermo* – calculated combustion temperature (excluding the nitriding reaction); Q – calculated heat release

The results of this study present investigations of SHS mixtures consisting of Al, Al_2O_3, $KClO_4$, MgO in a nitrogen atmosphere with an initial pressure of 5 MPa. To increase the combustion temperature, an oxidizer—potassium perchlorate $KClO_4$—was added to the initial mixture. Self-propagating high-temperature synthesis (SHS) was proposed as a synthesis method. This method utilizes the principle that the combustion reaction is initiated by external heat release, but after ignition, the process becomes self-sustaining due to intense heat release as a result of the exothermic reaction itself. The SHS method offers advantages such as short synthesis times and low energy consumption. Thus, SHS offers an alternative to the traditional synthesis of MgAlON.

The macrokinetic combustion parameters of the two main heat-generating factors—nitriding and oxidation—were studied. Figure 1 (a) presents the results of a thermodynamic calculation for mixtures with varying amounts of aluminum involved in the oxidation reaction, along with heat release calculations and experimental data. According to the obtained data, the adiabatic combustion temperature changes from 1140 to 1870 ºC. With an increase in aluminum content by 1 wt.%, the adiabatic combustion temperature increases by an average of 180 ºC, while the experimental value increases by ~100-120 ºC. The calculated heat release changes by ~28 kJ/mol.

Calculations were also performed with varying amounts of Al involved in the nitriding reaction (Fig. 1(b)). According to the obtained results, the adiabatic combustion temperature changes from 715 to 1280 ºC. With an increase in aluminum content, the adiabatic temperature increases by an average of 100 ºC, while the experimental value varies within very narrow limits. This can be explained by the insufficient initial pressure of nitrogen gas in the experiments, which leads to nitrogen filtration into the reaction zone, thereby limiting the combustion process. The calculated heat release changes by 11-12 kJ/mol for every 1% change in the amount of nitrided aluminum.

It was found that oxidation has a greater effect on the temperature and combustion rate, indicating its significant contribution to the synthesis of magnesium-aluminum oxynitride. Thermodynamic calculations indicate that the limiting reaction of nitriding occurs when gas is transferred to the synthesis zone (fig. 1). X-ray phase analysis of the combustion products of the mixtures was also conducted, with MgAlON present as the main phase in all products (fig. 2). However, potassium chloride (KCl) is also present as a secondary phase in the combustion products, which is not a significant concern, since during subsequent sintering of the samples, potassium chloride still evaporates before the materials are sintered.

Compact ceramic materials were sintered from single-phase magnesium-aluminum oxynitride powder materials by free sintering at a temperature of 1930 °C for 10 hours. The maximum values of hardness and Young's modulus were 32.1 ± 2 GPa and 330.6 ± 29 GPa.

This research was funded by Russian Science Foundation, grant number 24-79-00289.

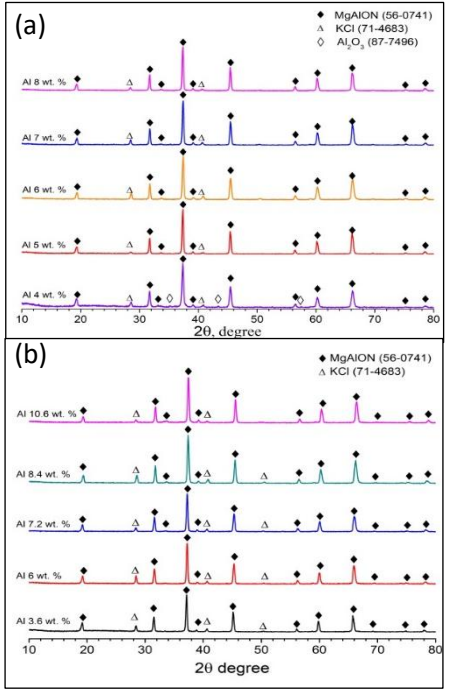

Fig. 2. Phase composition of combustion products with different Al content participating in the oxidation reaction (a) and in the nitriding reaction (b)

VII International School-Conference "Promising multicomponent ("high entropic") materials", dedicated to the 100th anniversary of Yuri Alexandrovich Skakov
October 06-10, 2025 г.

№3.13

APPLICATION OF ADDITIVE TECHNOLOGIES IN THE SYNTHESIS OF HIGH-ENTROPY COMPOUNDS AND COATING BASED ON THEM

Samodurova M.N., Polyakova M.A., Pashkeev K.Yu., Trofimova S.N.,
Latfulina Yu.S., Myasnikova A.A., Naprimerova E.D.

E-mail: samorovamn@susu.ru

As part of the study, new methods for producing non-metallic and intermetallic high-entropy compounds and coatings based on them using additive technologies were developed.

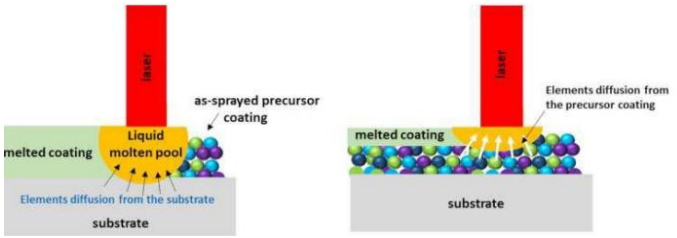

Fig. 1. Laser melting of a powder coating with partial melting of the substrate and without melting of the substrate

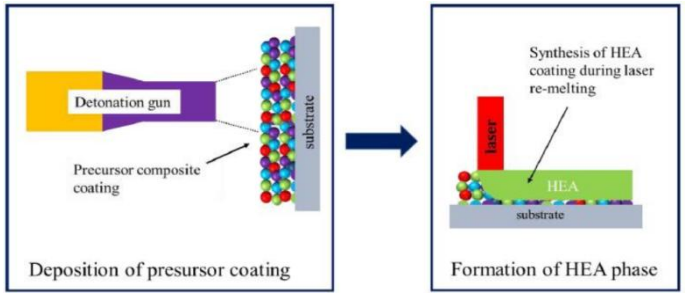

Fig. 2. Two-step approach to forming a high-entropy coating: application of a coating using the detonation spraying method followed by laser remelting

This work was supported by the Russian Science Foundation and the Government of the Chelyabinsk region, grant No. 23-19-20054, https://rscf.ru/project/ 23-19-20054/

The work aimed to create materials with a unique property profile for aerospace and engineering applications. Using three additive methods—laser cladding, cold spray, and detonation spraying—over 120 coatings were produced on steel, aluminum, and glass substrates. Both pre-synthesized high-entropy powders and in-situ synthesis from elemental mixtures were employed to form high-entropy intermetallic and oxide coatings. Comprehensive analysis (XRD, SEM, microhardness, wear, and thermal stability tests) confirmed that the methods produce coatings with strong adhesion and a stable phase structure.

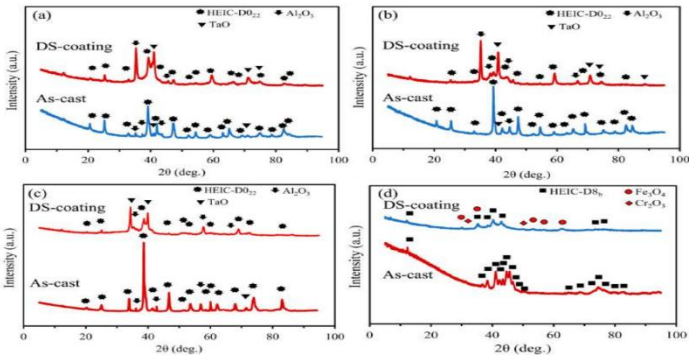

Fig. 3. XRD patterns of the (NbTaVCrTi)Al3 (a), (NbTaVNiFe)Al3 (b), (NbTaVZrHf)Al3 (c), and (FeNiCoCrMn)(MoCr) (d) HEICs in the as-cast and detonation spraying -coated states.

These models allow for the prediction of optimal process parameters and provide insight into the mechanisms of high-entropy phase formation under non-equilibrium conditions typical of additive manufacturing. The findings confirm the feasibility of engineering coatings with tailored functional properties and open new prospects for the application of additive technologies in the development of next-generation high-performance materials.

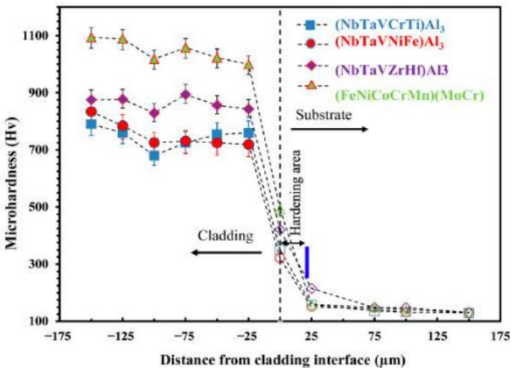

Fig. 4 Microhardness values recorded across the coating/substrate cross-section for (NbTaVCrTi)Al3, (NbTaVNiFe)Al3, (NbTaVZrHf)Al3, and (FeNiCoCrMn)(MoCr) high-entropy intermetallic compounds coatings.

VII International School-Conference "Promising multicomponent ("high entropic") materials", dedicated to the 100th anniversary of Yuri Alexandrovich Skakov
October 06-10, 2025

№ 3.14

Трибологическое поведение перспективных ультрамелкозернистых гетерофазных керамических композитов

С.К. Муканов, М.И. Петржик, Е.А. Левашов
Университет науки и технологий МИСИС, Москва, Россия
smukanov@misis.ru

Введение

Керамические композиционные материалы (ККМ) на основе тугоплавких нитридов, карбидов и боридов, несмотря на их высокую твердость, коррозионную стойкость, термическую стабильность, имеют склонность к хрупкому разрушению. Создание ультрамелкозернистых (УМЗ) ККМ, сочетающих высокую трещиностойкость, твердость, прочность, теплопроводность, термическую и химическую стойкость, низкие значения коэффициентов термического расширения и трения, расширит области применения в атомной энергетике, двигателестроении и других отраслях промышленности. Важным вопросом является поиск оптимальной концентрации, размеров и способа введения в порошковую смесь активаторов спекания, наноразмерных и субмикронных микродобавок с учетом их совместимости и возможностью химического взаимодействия с керамической матрицей.
Целью настоящей работы являлось исследование трибологических свойств перспективных ККМ на основе карбидов и нитридов титана и тантала

Материалы

Система	Матрица	Добавки	Трещиностойкость (K_{IC}), МПа·м$^{1/2}$
TiSiCN	c–Ti(C,N); β-Si_3N_4; c–SiC	YAG; h–BN	4,5–5,7
TaSiN	h–TaN; β-Si_3N_4; c–TaN	YAG; h–BN; VGO	5,4–9,3
TaSiCN	c–Ta(C,N); β-Si_3N_4	YAG; h–BN	6,2–8,5
TiC-Cr_3C_2	TiC; Cr_3C_2; Ni	–	4,8–7,8

Методы

Схема «стержень-диск» (ASTM G99-23)
Контртело: шарик, Ø3 мм (Al_2O_3 / Сталь)
Нагрузка: 5 Н
Линейная скорость: 0,3; 0,6; 0,8 м/с
Среда: воздух / масло

Объём изношенного материала определяли с использованием оптического профилометра WYKO NT1100 (Veeco, США).

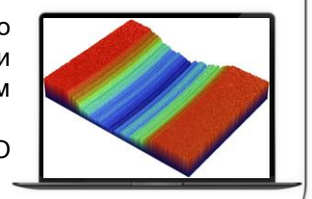

Испытания при сухом трении

Обнаружено, что при высокой скорости (0,8 м/с) ККМ на основе TiC-Cr_3C_2 и TiSiCN демонстрируют низкие значения коэффициента трения (0,25–0,55) и приведенного износа (≤2×10^{-6}·мм^3/Н·м). Напротив, керамики TaSiN и TaSiCN обладают более высокими значениями коэффициента трения (0,70–0,79) и приведенного износа (≤13×10^{-6} мм^3/Н·м). Благоприятные трибологические характеристики титансодержащей керамики обусловлено образованием субмикронных продуктов износа со структурой рутил.

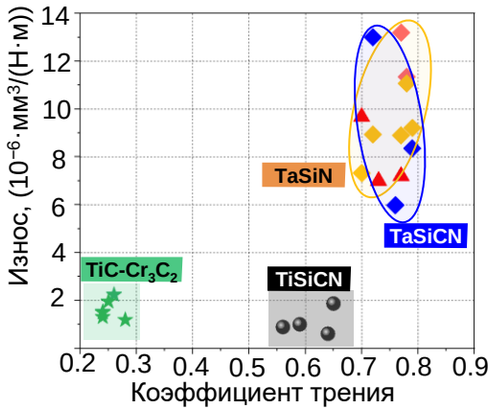

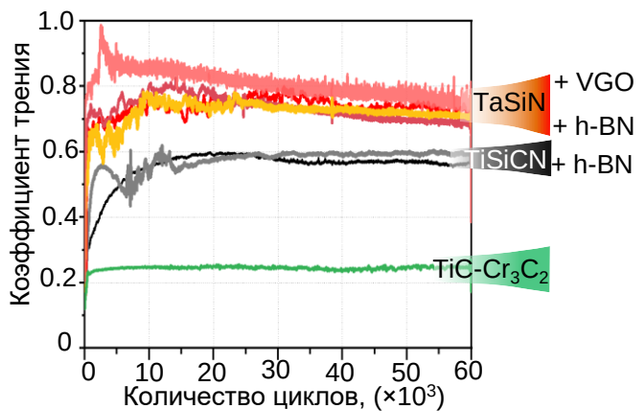

Испытания в масле

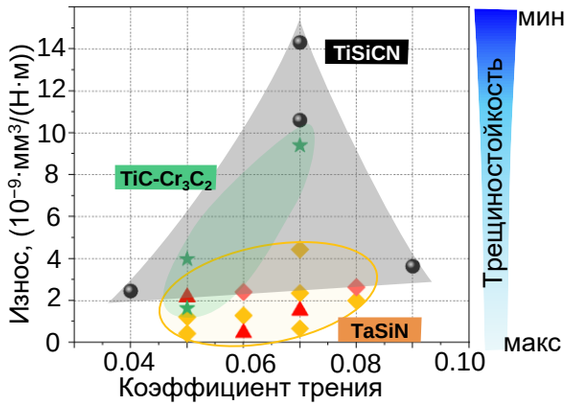

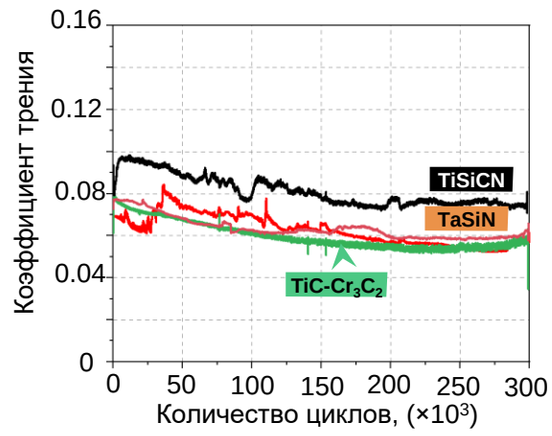

Исследование продуктов износа

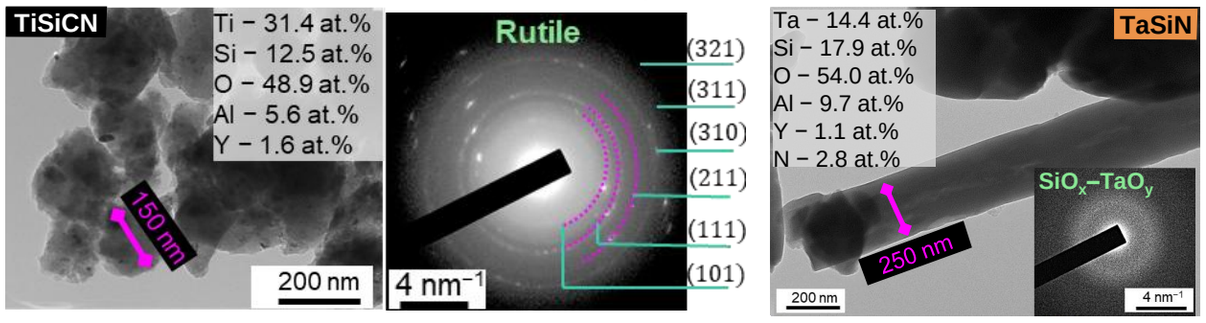

Независимо от состава, ККМ характеризуются узким диапазоном установившегося коэффициента трения (0,03–0,10). При отсутствии условий для реализации окислительного механизма износа, т.е. в условиях смазки и при низких скоростях, определяющим фактором трибологического поведения керамик является их трещиностойкость. Вырывание зерен приводит к локальному разрушению смазочной плёнки, что сопровождается увеличением коэффициента трения и интенсивности изнашивания. Введение функциональных добавок (YAG, h-BN, VGO), повышающих трещиностойкость, препятствует хрупкому разрушению зерен и тем самым обеспечивает рост износостойкости ККМ в условиях смазки.

Работа выполнена при финансовой поддержке Министерства науки и высшего образования РФ в рамках государственного задания (проект FSME–2025–0003).

VII International School-Conference "Promising multicomponent ("high entropic") materials", dedicated to the 100th anniversary of Yuri Alexandrovich Skakov
October 06-10, 2025 г

№ 3.15

KochuraEG@mail.ru

LASER DIRECTED ENERGY DEPOSITION OF A REFRACTORY NbTaV COMPLEX CONCENTRATED ALLOY USING ELEMENTAL POWDERS: MICROSTRUCTURE AND MECHANICAL PROPERTIES

Kochura E.G.*, Krasanov I.V., Yurchenko N.Yu.
Saint-Petersburg State Marine Technical University, 190121 Saint Petersburg, Russia

Particle morphology and size distribution of the NbTaV powders

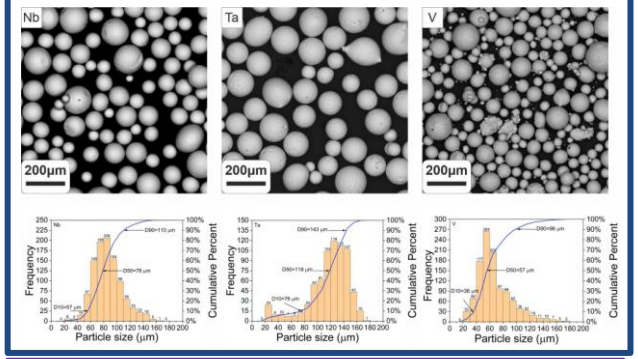

Sample deposition scheme

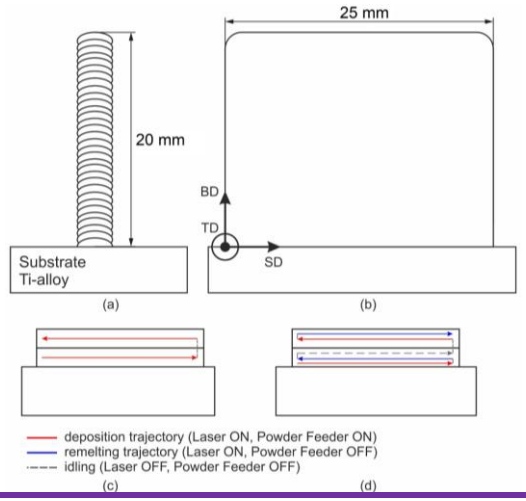

Microstructure

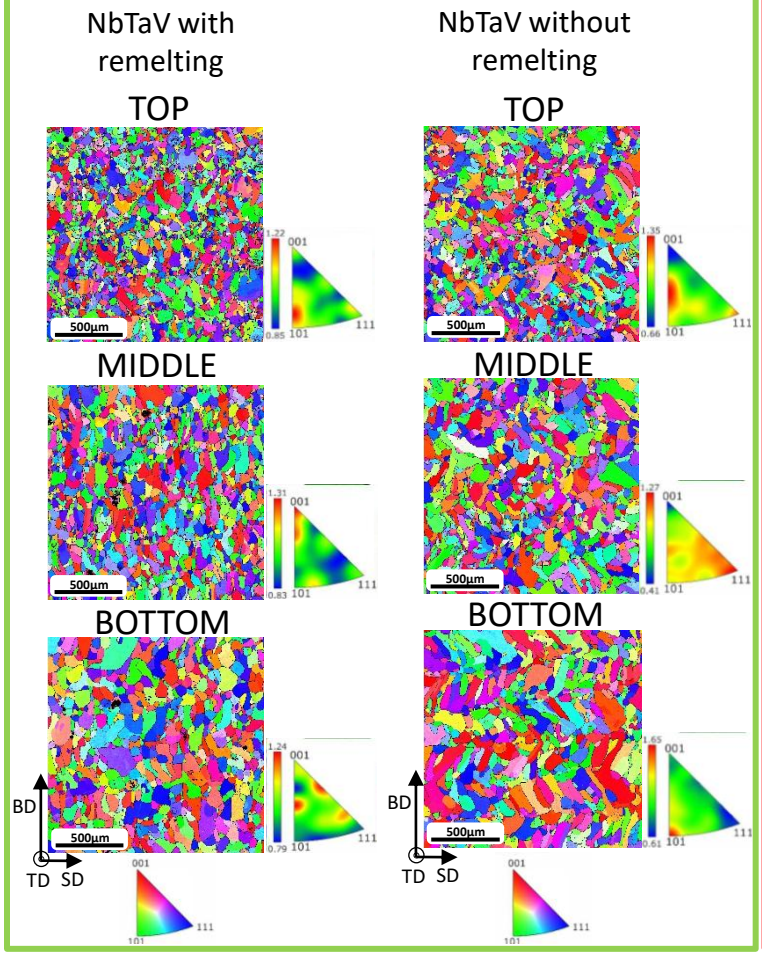

Mechanical properties

Engineering stress-strain and true stress/strain hardening rate-true strain curves

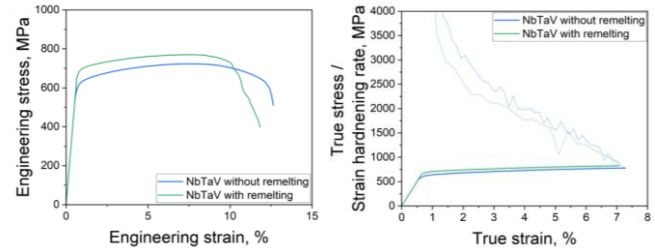

EBSD-IPF-KAM images of the NbTaV

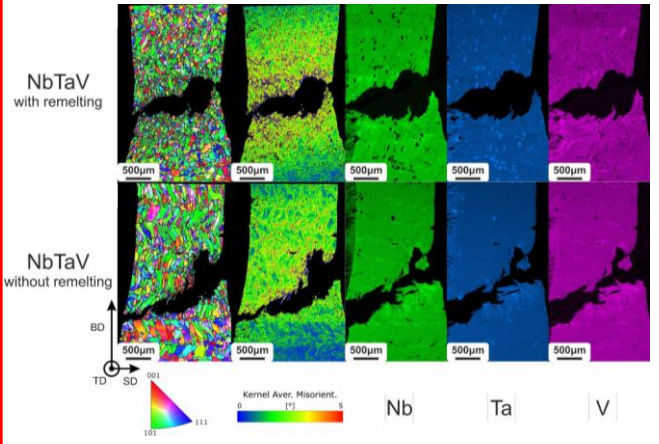

This work was supported by the Russian Science Foundation Grant no. 25-79-30012 (https://rscf.ru/en/project/25-79-30012/).

VII International School-Conference "Promising multicomponent ("high entropic") materials", dedicated to the 100th anniversary of Yuri Alexandrovich Skakov
October 06-10, 2025 г.

№3.16

DEVELOPMENT OF NICKEL-BASED SUPERALLOYS FOR ADDITIVE MANUFACTURING

Astakhov I.I[a,b], Klimova M.V[a,b], Klimenko D[a,b], Stepanov N.D[a,b]
[a]Institute of Laser and Welding Technologies, State Marine Technical University, Saint Petersburg, Russia
[b]National Research University "Belgorod State University"(BelSU) Belgorod, Russia
Astakhov@smtu.ru

Modeling of new alloys

Element	Ni	Al	Co	Cr	Ti	Mo	W	C	Fe	B	Si	Mn
ZhS6K	bal	5,51	4,59	10,75	2,96	4,07	5,80	0,15	-	-	-	-
Concentrations	bal	4-7	3-6	8-13	2-4	3-5	4-6	0,1-0,2	1-3	0,01	0,1	0,1
Step	-	1	1	1	1	1	1	0,1	1	-	-	-

Thermo-Calc Software + python

14289 alloys

73 clusters

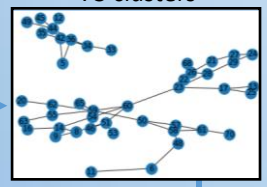

- Reduced solvus temperature of the γ' phase.
- High volume fraction of γ' phase at 950˚C
- Reduced volume fraction of other intermetallic and ceramic second phases.
- The crystallization interval is no more than 65˚K

Ni70

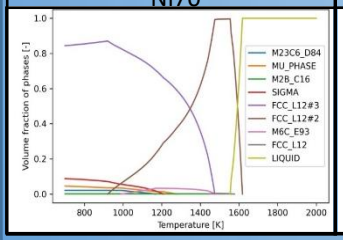

Ni75

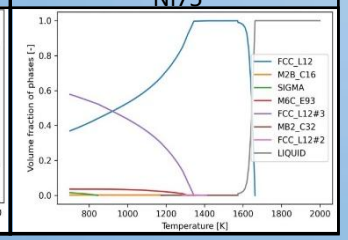

Structure

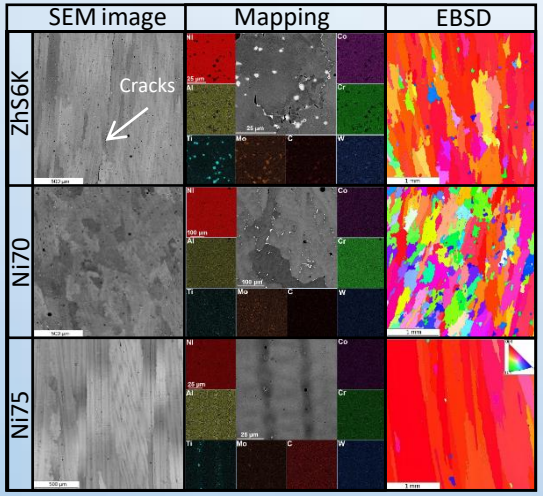

Morphology γ'-phase

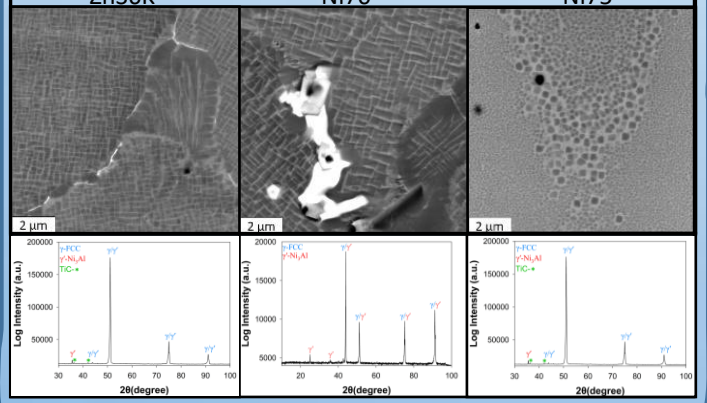

Mechanical properties

Stress-strain curves

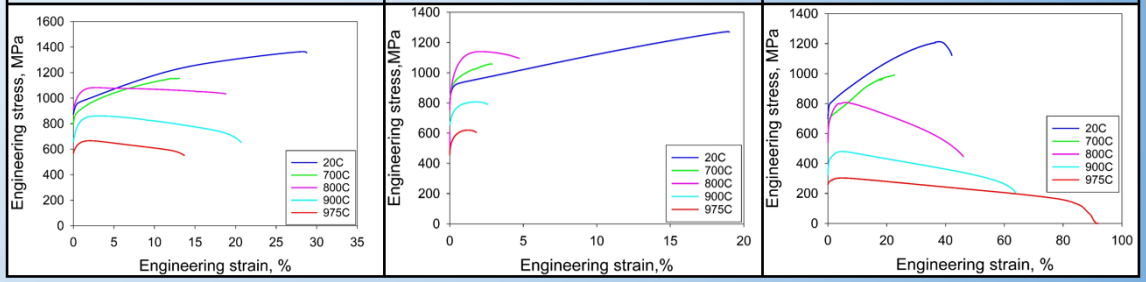

Mechanical properties of alloys obtained by the DLD method in the temperature range of 25°C-975°C

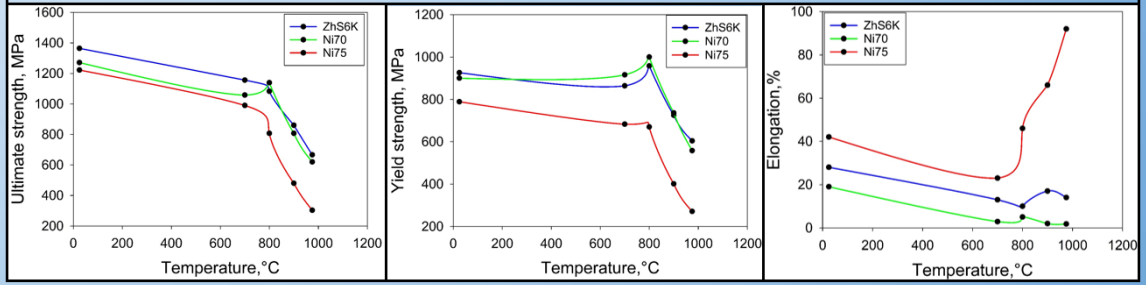

Conclusions

In this work, a new compositions of superalloys based on ZhS6K were designed using high-performance CALPHAD calculations. The microstructure studies confirmed the absence of cracking in the modified alloys compared to ZhS6K, which indicates better manufacturability. A comparison of the mechanical properties with the ZhS6K alloy showed that the developed alloys has slightly lower strength characteristics than the ZhS6K alloy. However, the ductility of NI75 was higher, for example, at a temperature of 975°C, the elongation under tension was 6 times greater than that shown by the ZhS6K alloy (14%). At the same time, Ni70 showed the best strength properties at 800°C, the ultimate strength and yield strength were 1139 and 1000MPa, respectively.

*The reported study was funded by the Ministry of Science and Higher Education of the Russian Federation (Grant Agreement No. 075-15-2025-006 dated February 26, 2025).

VII International School-Conference "Promising multicomponent ("high entropic") materials", dedicated to the 100th anniversary of Yuri Alexandrovich Skakov
October 06-10, 2025 г.

№ 3.18

st063188@student.spbu.ru

INFLUENCE OF THE ULTRASONIC ASSISTANCE DURING WIRE ARC ADDITIVE MANUFACTURING ON THE GRAIN SIZE IN THIN WALL AND THICK MULTI-ROWS STEEL SAMPLES

S. Belyaev[1], V. Rubanik[2], V. Rubanik jr.[2], N. Resnina[1], M. Starodubova[1], D. Drabo[2]
[1]Saint-Petersburg State University, Saint-Petersburg, Russia
[2]Institute of Technical Acoustics, National Academy of Science of Belarus, Vitebsk, Belarus

Aim of the study

To investigate the influence of the ultrasonic (US) assistance on the grain size in the samples produces by the wire arc additive manufacturing (WAAM).

Thin wall samples were prepared in 3 regimes:

- without US (WAAM)
- under US during deposition of the layer and during inter-pass cooling (WAAM+USV-1)
- under US during deposition of the layer only (WAAM+USV-2)

Thick multi-rows samples were prepared in 2 regimes:

- without US (WAAM)
- under US during deposition and inter-pass cooling (WAAM+USV)

Conclusions

In thin wall the columnar grains were observed only in top layers.
In thick samples the columnar grains were found in all layers.
The US assistance during WAAM decreased the length of the columnar grains.

Thin wall sample

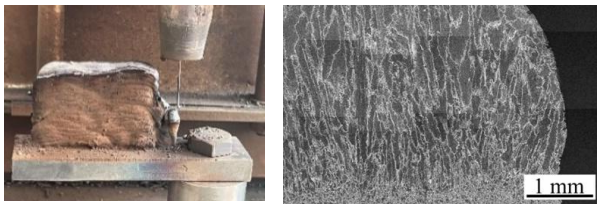

Image of the WAAM+USV-1 sample with 36 layers, the view of the columnar grains in the upper part of the sample

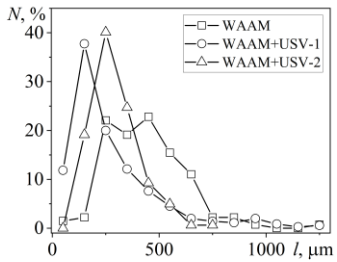

The distribution of the length of the grains in the upper part of the sample

Thick multi-rows sample

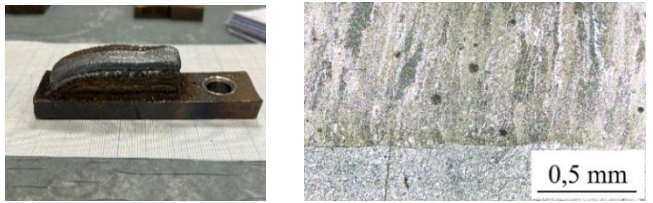

Image of the WAAM sample, the view of the columnar grains with substrate at the bottom

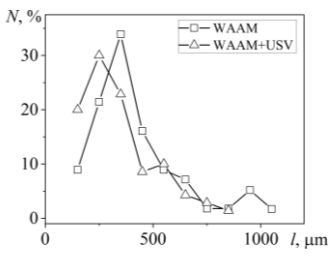

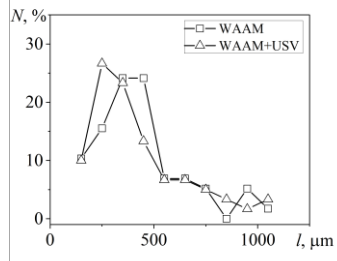

The distribution of the length of the columnar grains in the upper part and the middle of the sample

The study was financially supported by joint project of the St.Petersburg Science Foundation (grant number 23 RB-09-43) and the Belarus Republican Foundation for Fundamental Research (grant number T24SPbG-008).

VII International School-Conference "Promising multicomponent ("high entropic") materials", dedicated to the 100th anniversary of Yuri Alexandrovich Skakov
October 06-10, 2025 г.

№ 3.20

CARBIDE PARTICLES FORMATION IN MELTS BASED ON HIGH-ENTROPY ALLOYS: MODELING AND EXPERIMENTAL STUDY

Bodrov E., Mikhailov D.V., Shabalina D.A., Efimova M.E.,
Rybalchenko K.G., Samodurova M.N., Trofimov E.A.

E-mail: trofimovea@susu.ru

This study explores cost-effective alternatives to conventional cobalt-based stellites using high-entropy alloy (HEA) principles. The research focused on M(Cr30W5C1.5) systems, where "M" is a combination of one to four elements from Fe, Ni, Co, Al, Cu, and Mn. The goal was to develop materials with performance comparable to stellites by creating a multi-element matrix without a single dominant element.

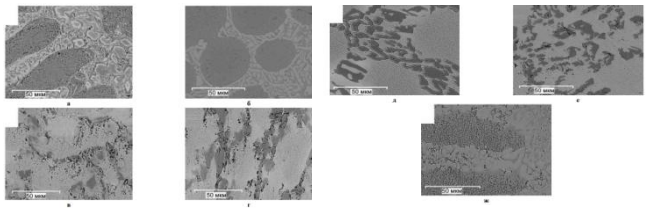

Fig. 1. Microstructures of cast samples at magnifications ×900, ×1000:
а — AlCoNiFe(Cr30W5C1.5); б — Al2CoNiFe(Cr30W5C1.5);
в — MnCoNiFe(Cr30W5C1.5); г — CoNiFe(Cr30W5C1.5);
д — Co(Cr30W5C1.5); е — Ni(Cr30W5C1.5); ж — Fe(Cr30W5C1.5)

The research employed a combined theoretical and experimental approach. Alloy samples were synthesized by vacuum induction melting of pure elements in corundum crucibles.

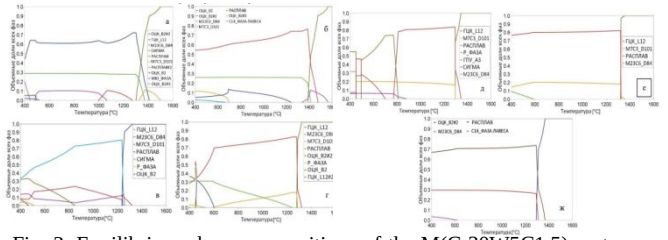

Fig. 2. Equilibrium phase compositions of the M(Cr30W5C1.5) systems in the range of 400–1600°C: а is AlCoNiFe(Cr30W5C1.5);
б is Al2CoNiFe(Cr30W5C1.5); в is MnCoNiFe(Cr30W5C1.5);
г is CoNiFe(Cr30W5C1.5); д is Co(Cr30W5C1.5)/Stellite 6;
е is Ni(Cr30W5C1.5); ж is Fe(Cr30W5C1.5)

Thermodynamic simulations were performed using Thermo-Calc software. Calculations included both equilibrium (CALPHAD) and non-equilibrium (Scheil) solidification models to predict phase composition and temperature-dependent volumetric behavior of the alloys.

For experimental characterization, scanning electron microscopy (SEM) coupled with energy-dispersive X-ray spectroscopy (EDS) and X-ray powder diffraction (XRD) were used to analyze the microstructure and phase composition. The high-temperature oxidation resistance, hardness, and mechanical strength of the alloy samples were also evaluated.

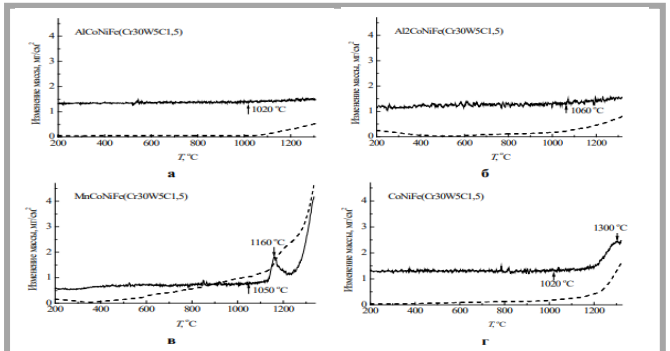

Fig. 3. Results of oxidation study of samples with multi basic matrix:
а — AlCoNiFe(Cr30W5C1.5); б — Al2CoNiFe(Cr30W5C1.5);
в — MnCoNiFe(Cr30W5C1.5); г — CoNiFe(Cr30W5C1.5)

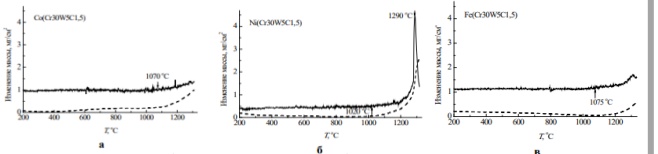

Fig. 4. Results of oxidation studies of samples based on individual elements of the iron subgroup: а — Co(Cr30W5C1.5);
б — Ni(Cr30W5C1.5); в — Fe(Cr30W5C1.5)

The study showed that alloy properties can be optimized by adjusting the matrix composition and heat treatment. A strong correlation was found between the phase composition, carbide morphology, and functional properties. The resulting materials combine high hardness, excellent heat resistance, and reduced cobalt content, making them cost-effective candidates for extreme operational conditions.

The work was supported by Russian Federation represented by the Ministry of Science and Higher Education of the Russian Federation, project number (contract number) No. 075-15-2022-1243.

VII International School-Conference "Promising multicomponent ("high entropic") materials", dedicated to the 100th anniversary of Yuri Alexandrovich Skakov
October 06-10, 2025 г.

№ 3.25

E-mail klopotovaa@tsuab.ru

EVOLUTION OF THE STRUCTURAL STATE OF THE HIGH-ENTROPY ALLOY TiNbZrTaHfCu$_x$

Abzaev Yu.A., Klopotov A.A., Prokopenko N.A., Petrikova E.A., Guda S.A., Ivanov Yu.F.
Tomsk State University of Architecture and Building, Tomsk, Russia
Institute of High Current Electronics, Tomsk, Russia

The aim of the present work is to investigate the evolution of structure and phase composition in thin (2…3 μm) TiNbZrTaHfCu high-entropy alloy (HEA) films using a crystallographic reference database generated by the evolutionary code USPEX, to determine quantitative phase content via the Rietveld method, and to calculate phase stability parameters using first-principles methods (DFT) in the CASTEP code. The primary emphasis is placed on studying crystal lattice stability via Miedema's method, phase evolution, and their energetic states as a function of deposition duration.

Film formation was carried out by deposition from a multi-element gas-metal plasma, generated by simultaneous vacuum-arc evaporation of TiNbZrTaHf and Cu composition cathodes in a plasma-assisted mode (Ar). Experiments on the deposition of multi-element films were conducted on the VUIPS-1 setup. The process of thin film structure formation in situ with high temporal resolution was studied using a synchrotron radiation source – the VEPP-3 electron storage ring, BINP SB RAS. X-ray diffraction pattern acquisition and recording were performed continuously every minute for 155 minutes.

It has been established that increased deposition time induces a transition from metastable orthorhombic phases (*Amm*2, *Pmm*2) to the thermodynamically stable tetragonal phase I4mm.

The key role of Cu–Hf pairwise interaction in stabilizing the alloy has been revealed, compensating for the local instability of Zr–Cu and Ti–Cu pairs. It is shown that prolonged deposition reduces the enthalpy of mixing and Gibbs free energy, resulting in the formation of a homogeneous structure with >98% *I*4*mm* phase fraction.

Fig. On-line diffraction patterns of TiNbZrTaHfCu$_x$ alloy films, besieged for a period of time: a) 40 minutes; b) 60 min; c) 110 min d) 143 min: 1 – experiment, 2 – model, 3 – intensity difference.

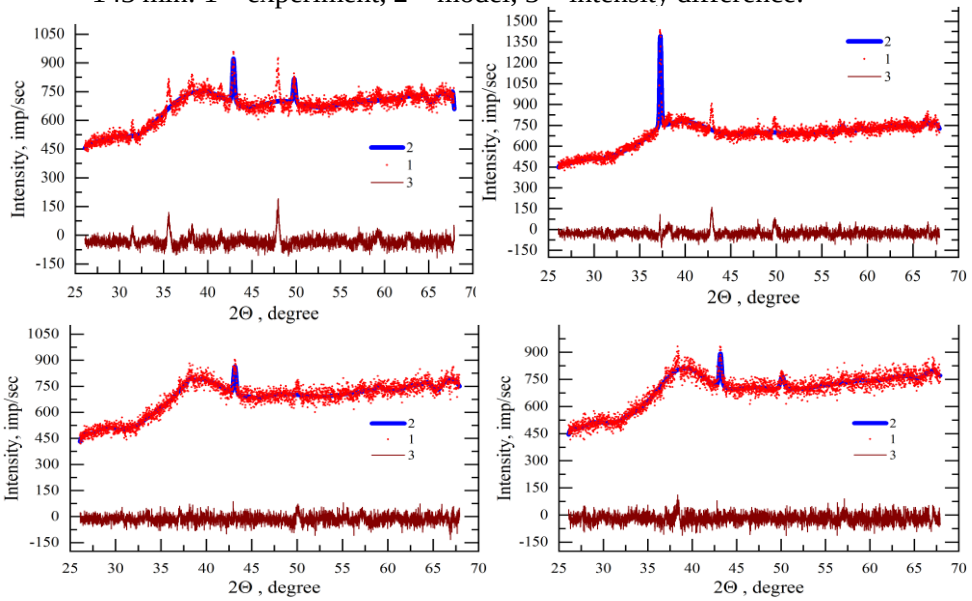

VII International School-Conference "Promising multicomponent ("high entropic") materials", dedicated to the 100th anniversary of Yuri Alexandrovich Skakov
October 06-10, 2025 г.

№ 3.25

dudova@bsuedu.ru

ON THE EFFECT OF HIGH TEMPERING TEMPERATURE ON THE CREEP RUPTURE STRENGTH OF A 10%CR STEEL

N.R. Dudova, R.V. Mishnev
Belgorod State National Research University, Belgorod, Russia

What is the upper limit of tempering temperature for 10%Cr martensitic steel to achieve high creep resistance at 650°C?

Normalization 1060°C +tempering 3 h

T 790

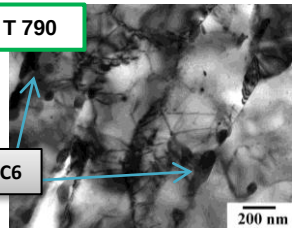

d_{lath} = 420 nm / ρ=1.3×10^{14} m^{-2}
d $M_{23}C_6$ = **104 / 110** nm

T 770

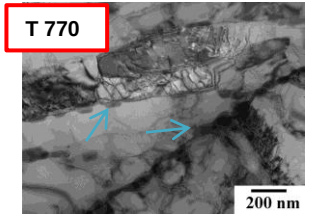

d_{lath} = 380 nm / ρ=1.7×10^{14} m^{-2}
d $M_{23}C_6$ = **66 / 73** nm

Creep tests at 650°C / 120-180 MPa

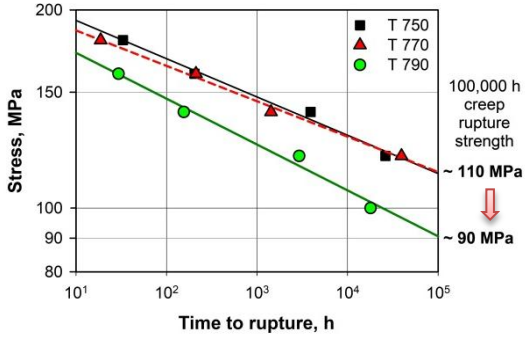

Higher tempering temperature of 790°C led to:
- a 20% decrease in the creep rupture strength

A power-law relationship

$$\dot{\varepsilon}_{min} = A\sigma^{n*}$$

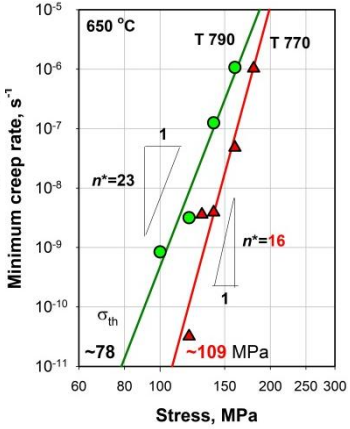

- a 30% lower threshold stress for creep (provided by $M_{23}C_6$ carbides, mainly)

Lower creep resistance is due to lower pinning of lath boundaries by $M_{23}C_6$ carbides (larger size / lower number density on boundaries)

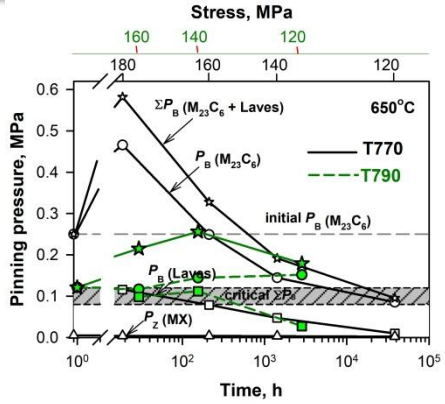

A higher tempering T=790 °C is not recommended for both short- and long-term creep strength.
T=770 °C is optimal.

VII International School-Conference "Promising multicomponent ("high entropic") materials", dedicated to the 100th anniversary of Yuri Alexandrovich Skakov
October 06-10, 2025 г.

№

NaumovStanislav@yandex.ru

STRUCTURE AND MECHANICAL PROPERTIES OF THIN-SHEET WELDED JOINTS OF HASTELLOY X ALLOY OBTAINED BY TIG WELDING WITH DIFFERENT FILLER MATERIALS BASED

S. V. Naumov[1], D. O. Panov[1], G. A. Salishchev1, D. S. Belinin[2], V. V. Lukianov[3]
[1]Laboratory of Bulk Nanostructured Materials, Belgorod State University, Russian Federation
[2]Perm National Research Polytechnic University, Perm, Russian Federation
[3]SPA «Technopark of Aviation Technologies», Ufa, Russian Federation

Thin-sheet structures of nickel-based heat-resistant alloys have a wide range application in the aerospace and energy industries. Hastelloy X (HX) is one of the most promising nickel-based heat-resistant alloys. Due to its exceptional corrosion resistance, HX is the preferred option for applications in difficult conditions. To obtain welded joints of the material, it is necessary to use available technologies and filler materials. Gas Tungsten Arc Welding (TIG) of nickel heat-resistant alloys is a wide spread technique. However, the choice of filler materials, and, consequently, welding modes for HX remains an urgent task. In this work, the possibility of obtaining thin-sheet welded joints by TIG welding using various filler materials is studied.

The optimal TIG welding modes are determined as follows: a base current of 10 A, a peak current of 15-30 A, a current modulation of 30%, and a pulse frequency range of 5-70 Hz. After welding, the joints are subjected to annealing at 1175-1120 °C for 30 min with water cooling.

The study reveals that, in the fusion zone, the Laves phase with a high Mo content dissolve. Laves phase particles of 1–5 μm in size in the fusion zone (in the interdendritic area) are formed. In the HAZ area, the line inclusions of the Laves phase remain, but subsequent heat treatment dissolves them both in the fusion zone and in the HAZ. When using ERNiFeCr-2 wire, the microhardness of the fusion zone is of 210±20 HV0.2, which is higher than the microhardness of the base metal (200±10 HV0.2). When using HN80 (CrNi80) wire, the microhardness of the fusion zone decreases to 180±20 HV0.2. Radiographic testing showed the absence of internal pores and cracks in the welded joints. The proposed technological recommendations for TIG welding with filler materials based on NiCr and NiFeCr alloys allow for the production of high-quality thin-sheet welded joints of HX.

This research was funded by the Russian Science Foundation, grant no. 19–79–30066.

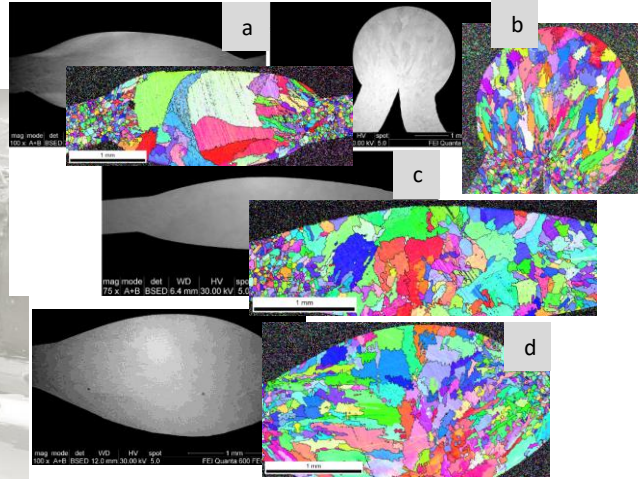

Figure 1. Cross-section of a weld seam of HX alloy obtained by TIG welding: a – with filler material NA718; b – without filler material; c – with filler material XH80, d – with HX strip

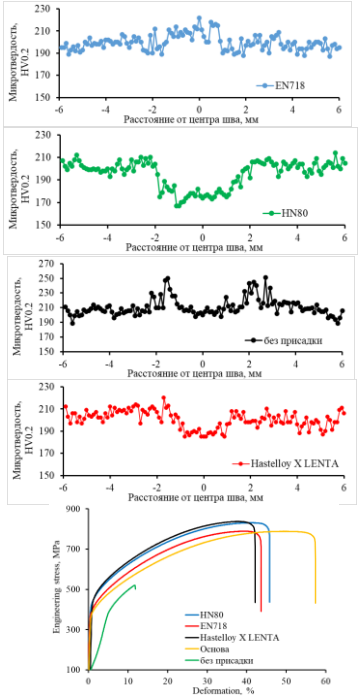

Figure 2. Mechanical properties of welded joints

VII International School-Conference "Promising multicomponent ("high entropic") materials", dedicated to the 100th anniversary of Yuri Alexandrovich Skakov
October 06-10, 2025 г.

№ 2.17

E-mail: vlasov_dyu@pfur.ru

Technological Features of Laser Cladding of Composite Coatings Based on Inconel 625/WC Alloy

Denis Vlasov[1,2], Ksenia Bazaleeva[1,2], Andrei Alekseev[2], Rustan Shipshev[2]
[1] Moscow Polytechnic University, Bolshaya Semyonovskaya str.38, 107023, Moscow, Russia
[2] Peoples' Friendship University of Russia named after Patrice Lumumba (RUDN University), Moscow, 117198, Russia

ЦЕЛИ И ЗАДАЧИ ИССЛЕДОВАНИЯ

Цель – повышение эксплуатационных характеристик композиционных покрытий Inconel 625/WC, синтезированных методом лазерной наплавки, путем варьирования технологических параметров процесса и *изменения структурного состояния исходного порошкового материала.*

Задачи:

1) разработка технологии лазерной наплавки бездефектных композиционных покрытий Inc 625/WC;

2) исследование зависимости фазово-структурного состояния композиционных покрытий Inc 625/WC от технологических параметров процесса;

3) исследование влияния фазово-структурного состояния покрытий на их
- механические характеристики;
- коррозионные свойства;
- термическую стабильность.

3D-принтер InssTek MX-Grande

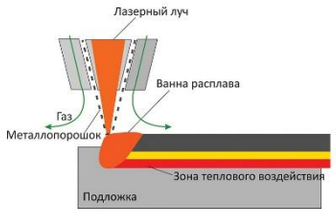

Схема и процесс лазерной наплавки методом прямого лазерного выращивания (ПЛВ).

ТЕХНОЛОГИИ ПОЛУЧЕНИЯ ИЗДЕЛИЙ С ЗАДАННЫМ УРОВНЕМ СВОЙСТВ ПРИМЕНИТЕЛЬНО К ТЕХНОЛОГИИ ПЛВ

Требования предъявляемые к геометрии валика:
1. Коэффициент формы валика $f = \frac{h}{L}$, должен находиться в диапазоне [0,2;0,33]
2. Коэффициент проплавления $d = \frac{S_p}{S_p+S_h}$, должен быть в диапазоне [0,1;0,4]
3. Ширина валика L в интервале от 1,7 мм до 3,0 мм при диаметре лазерного пятна 1,8 мм
4. θ – краевой угол у основания валика θ < 90°
5. Отсутствие трещин

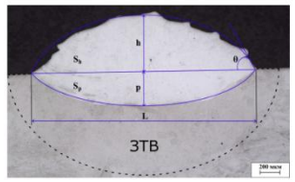

ХАРАКТЕРИСТИКИ ЕДИНИЧНЫХ СЛОЁВ

ΔXY – величина перекрытия между центрами соседних валиков. Рекомендуемое значение - ΔXY = 0,7L.

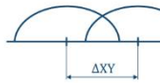

Структура монослоев, полученных методом ПЛВ со скоростью сканирования 1000 мм/мин, мощностью 1000 Вт и разным расстоянием между валиками: а – 0,5L; б – 0,7L; в – 0,9L

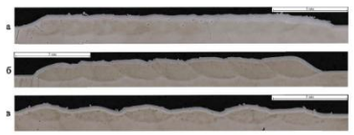

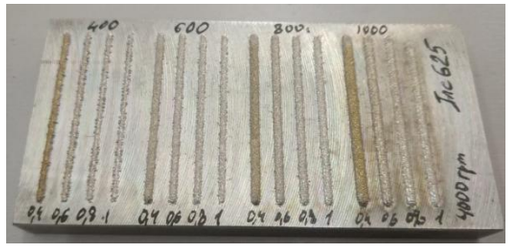

Единичные лазерные треки (валики) на подложке

Единичные слои из отобранных режимов на подложке

ИСХОДНЫЙ ПОРОШКОВЫЙ МАТЕРИАЛ

Состав матричного сплава Inconel 625

Элемент	Cr	Mo	Nb	Ni
Концентрация, мас.%	20.6	9.7	3.8	основа

Дифрактограмма порошка Inconel 625

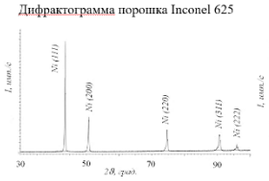

Дифрактограмма порошка карбида W

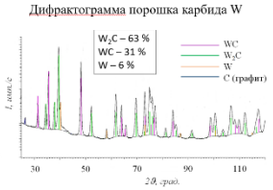

РЕЖИМЫ ЛАЗЕРНОЙ НАПЛАВКИ

P = 400 ÷ 2000 Вт
V = 400 ÷ 2000 мм/мин.
V_n = 30 ÷ 50 г/мин.
d = 1.8 мм
l = 0.7 L

P = 800 ÷ 1000 Вт
V = 600 ÷ 1000 мм/мин.
V_n = 30 г/мин.
d = 1.8 мм
l = 0.7 L

Режимы								
WC, об.%	10	20		30		40		50
P, Вт	1000	1000	800	1000	1000	1000	800	800
V, мм/мин.	800	800	800	600	800	600	800	600
P/V, Вт·мин./мм	1.25	1.25	1	1.67	1.25	1.67	1	1.33

СТРУКТУРА КОМПОЗИЦИОННЫХ ПОКРЫТИЙ

Панорама покрытия (металлографический анализ)

Металлографический анализ

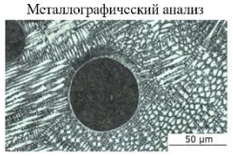

Растровая электронная микроскопия

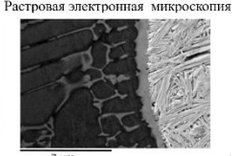

РАСПРЕДЕЛЕНИЕ ЭЛЕМЕНТОВ ПО СТРУКТУРЕ ПОКРЫТИЯ

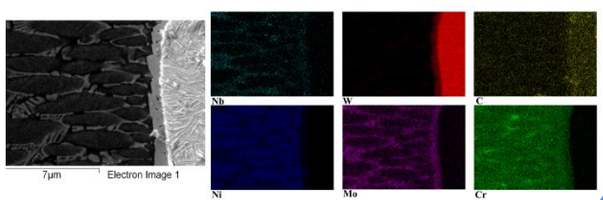

ВЛИЯНИЕ ПЛОТНОСТИ УДЕЛЬНОЙ ЭНЕРГИИ P/V

Дифрактограммы

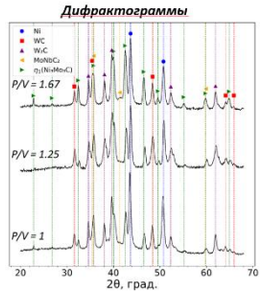

Период решетки (Ni)

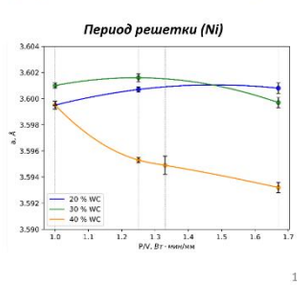

ВЛИЯНИЕ КОНЦЕНТРАЦИИ УПРОЧНЯЮЩЕЙ ФАЗЫ

Покрытия Inconel 625/(WC,W_2C)

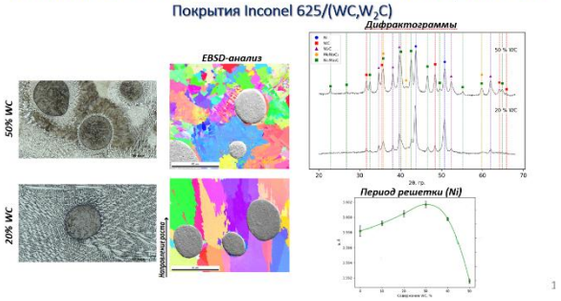

МИКРОТВЕРДОСТЬ МАТРИЦЫ ПОКРЫТИЯ

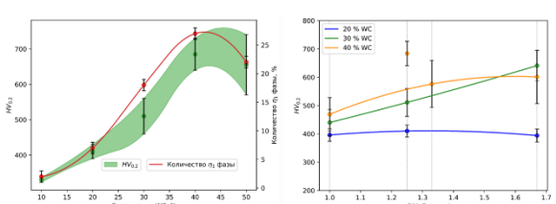

ВЫВОДЫ:

1. Доля карбидов зависит от энергии процесса: при большей энергии часть WC растворяется, меняется их распределение.
2. В покрытиях выявлены WC, W_2C, никелевый раствор и карбиды Ni_3Mo_3C, $MoNbC_2$, количество которых растёт с мощностью лазера.
3. РЭМ: Ni-Cr-Fe в матрице, W-C в карбидах, Mo и Nb сосредоточены вокруг карбидов.
4. Микротвёрдость повышается с ростом содержания WC; меньшая скорость сканирования при одинаковой мощности увеличивает твёрдость.